Comparison of the ground penetrating radar characterization of winter processes with the results of hydrological simulations

by

Jennifer Hansen

A thesis

presented to the university of waterloo

in fulfillment of the

thesis requirement for the degree of

Master of Science

in

Earth Sciences

Waterloo, Ontario, Canada 2014

Author's Declaration

I hereby declare that I am the sole author of this thesis. This is a true copy of the thesis, including any required final revisions, as accepted by my examiners. I understand that my thesis may be made electronically available to the public.

Jennifer Hansen

Abstract

Ground penetrating radar (GPR) is a useful tool to characterize and investigate a variety of cold region processes, including but not limited to permafrost development and glacial morphology. Despite a comprehensive coverage, with respect to permafrost and glacial morphology investigations, few if any previous studies have captured the long term seasonal trends of freezing and thawing cycles. This work introduces a new method for monitoring freeze/thaw processes by demonstrating the capacity of GPR to characterize the dynamic changes of the frost front and also identify thawing events that occur near the surface throughout the winter season. This study incorporates two full winter seasons, October 2006 to April 2008 to capture the distinct freezing and thawing cycles that occur during these times. These winter seasons were surveyed by Steelman et al., (2012) and the data collected during their study is incorporated into this work. These surveys contain high resolution, 900 MHz surveys, consisting of common midpoint sounding (CMP) and reflection profiles. These high resolution reflection profiles precisely imaged the location of the frost front throughout the winter season to provide 'real time' data on the frozen state of the ground. CMP soundings collected by Steelman et al., (2012) also provide the ability to calculate accurate depth estimates of the interface between the frozen and unfrozen zone along with contributing electo-magnetic (EM) wave velocity estimates that indicate the relative quantity of unfrozen water in the ground. Oscillations in frost front depth were observed that correlated well with temperature trends, descending deeper in the soil column during colder periods and retreating during warmer periods of the winter season. Moreover, near surface and complete thaws were documented by the appearance of dispersive wave guides. This high resolution GPR data set from 2007-2008, provides a thorough description of the winter processes, which were constrained by comparison to an unsaturated heat transport flow model, HYDRUS 1-D. Using laboratory-derived hydraulic properties and industry accepted heat transport values along with limited parameter calibration, good agreement was achieved between the HYDRUS 1-D model results and the observed values. The weighted root mean square error (RMSE) is 0.07 m, showing the ability the HYDRUS 1-D model has to represent the field data and how on average there is little error between the observed GPR field data and predicted HYDRUS 1-D model results. Moreover the model captures the general oscillations and trends in the frost front which shows good predictability for the model. The HYDRUS 1-D model was validated using GPR data collected from the 2006-2007 survey year. Although this latter data set

is somewhat less robust, the model is still able to capture the general frost movement trends and further demonstrate its ability to simulate GPR interpreted freeze/thaw dynamics.

Contents

List of Figures

List of Tables

Chapter 1: Introduction

1.1 Background

As pore water begins to freeze under the influence of freezing temperatures, it can alter the soil structure of the subsurface and produce observed changes to the local hydrology of an area (Nyberg et al., 2001; Woo and Winter, 1993; Keith et al., 1999; Ding et al., 2000). Changes to the hydrology of a catchment due to the onset of freezing, can have compounding effects. The hydrology of an area can control, to an extent, groundwater flow regimes, recharge, and the micro-ecology of soils, (Fitzhugh et al., 2001; Marlon, 1995; Winter 1998). Moreover, freezing and thawing cycles are intimately linked to surface energy budgets and consequently climate change. Changes to freezing and thawing long-term seasonal trends have been shown to be an indicator for shifts in climate regimes (Solomon et al., 2007). Thus, preserving the expanse of the cryosphere relies on how the changing climate will affect long-wave radiation and precipitation of the Northern latitudes, which currently is poorly understood. Changes to the duration and magnitude of freeze thaw cycles have already been observed worldwide (Solomon et al., 2007). For instance, changes in seasonally frozen ground in Russia with a reduction in frost depths of 0.34 m from 1956 to 1990 due to an increase in snow depths have been observed as well as a decrease in the Tibetan Plateau of 0.05 m to 0.22 m from 1967 to 1997 and an overall 7% decrease in the Northern Hemisphere from 1901 to 2002 (Frauenfeld et al., 2004; Zhao et al., 2004; Zhao, Cheng and Li, 2003; Solomon et al., 2007). Figure 1.1 illustrates the areal extent of seasonally frozen ground including the active layer in permafrost areas (Duguay et al., 2005).

Despite the expansive scale of the cryosphere and how freeze/thaw cycles can strongly influence other aspects of the hydrologic system, research in this area is lacking and may be attributed to how difficult it is to measure and estimate the areal extent of the frost zone under snow packs and the ground (Ireson et al., 2013; Henry, 2007; Woo et al., 2000). Moreover, the current manner by which scientists and engineers measure water and ice contents during freezing is inadequate, as the level of detail required to study these processes is beyond the detection limit of these instruments and methods, such as thermistors and time-domain reflectometers (TDR) (Ireson et al., 2013; Iwata et al., 2010). When reviewing the literature it is evident there is a gap in the holistic understanding of frost related hydrologic processes, indicating that there is a need for a better way to monitor these systems. Developing new techniques to describe the physics of

these systems through governing equations is a step in the right direction. Developing new techniques will provide model developers with the foundation to create numerical heat transport and flow models that can simulate the near-surface freeze-thaw cycles and the underlying vadose and groundwater processes. One method currently does not exist that can explicitly perform this function (Ireson et al., 2013). Having a numerical freeze/thaw and flow model that can rigorously and accurately predict different climate scenarios would be extremely beneficial to understanding the impacts climate change will have to the cryosphere.

A wide variety of sensors and methods have been developed to attempt to capture the many entangled processes related to freeze thaw cycles; however, none have been successful at providing the necessary information researchers require to properly characterize these events (Ireson et al., 2013). There are a variety of point source temperature sensors which rely on dimensional, chemical or electrical changes that are currently used to locate the zero temperature isotherm which can be used to delineate certain frost related boundaries; Table 1.1 lists these and other instruments and their accuracies. One problem related to using thermometers and frost tubes are that they must be in contact with the soil in order to measure the temperature. Thus, different procedures for using these instruments include extracting soil by means of drilling and directly measuring the soil temperature of the extracted soil or installing the instrument into the ground and monitoring ground temperature continuously. Both methods have problems; for instance when extracting soil from the ground to measure soil temperature, the soil temperature may change to equilibrate with the ambient air or different drilling fluids used can change the temperature of the ground due to the friction generated during drilling (Krzewinski et al., 1985). Moreover, these instruments only measure soil temperature and provide no information about the characteristics of the frozen zone. This inability to directly measure the quantity of interest can lead to experimental artefacts because water in the subsurface does not freeze at precisely 0°C due to different solutes and latent heat transfer. Thus, engineers and scientists using the 0°C isotherm to locate the bottom of the frost zone may be misrepresenting the system (Krzewinski et al., 1985). In summary, these more conventional methods are invasive, point source techniques that require numerous horizontally and vertically positioned probes at many depths. These invasive methods also tend to be unsuitable for large-scale investigations due to their higher costs and inability to ascertain the true subsurface characteristics due to their intrusive and indiscreet method of measurement.

A number of different lab techniques have also been used to study freeze thaw cycles. These techniques usually consist of incubators, or growth chambers, which are set up to simulate winter conditions, by way of temperature, frost and flow simulations. Henry, (2007) reviews a number of these studies to highlight the methodological weakness of these lab techniques and suggests improvements for researchers studying freeze thaw cycles. A major problem noted by Henry, (2007) is that there is little conformity between studies in terms of how they choose to conduct freeze thaw experiments. This lack of consensus has diminished the relevance of many of these studies because results are skewed by experimental artefacts (Henry, 2007). In general, one reason it is difficult to represent actual field soil temperature conditions in the lab because lab experiments typically use small soil cores which equilibrate to temperatures more quickly than in a field setting. Thus, lab-derived results may exaggerate freeze thaw effects. Another problem Henry, (2007) points out are the number and frequency of freeze-thaw cycles employed by most laboratory studies is typically less than five (Henry, 2007). In the context of climate change, the number of freeze/thaw cycles over a cold season, especially near the surface, is likely to increase (Solomon et al., 2007). In only considering a few freeze/thaw cycles, these earlier studies may not have properly captured the cumulative effects of the numerous freeze-thaw cycles that can occur across a typical cold season. These identified weaknesses in lab-based studies suggest that field studies may be a better alternative. However, it needs to be re-emphasized that more work needs to be done to develop a consensus among scientists regarding the best way to conduct these experiments in a more comprehensive manner.

Geophysical methods have also been used widely in the characterization and investigation of seasonally frozen areas. Specifically, instruments relying on the dielectric permittivity of soils to characterize their properties have been used extensively in this field (Boike and Roth, 1997; Hinkel et al., 2001; Kneisel et al., 2008). Time domain reflectometry (TDR) and ground penetrating radar (GPR) respond well to contrasts in dielectric permittivity κ; and the greater the contrast the greater, the amplitude of the reflected pulse (Cassidy, 2009). There is a large contrast between the dielectric permittivity of ice and water ($\kappa_{ice} = 3.2$, $\kappa_{water} = 80$), thus TDR and GPR are ideal for the study of cryotic soils (Kneisel et al., 2008). TDR has been shown to be able locate the frozen/unfrozen interface by measuring the produced reflections reflected from the frost front (Baker et al., 1982). The accuracy of this method is comparable to those

measurements associated with locating the 0°C isotherm (Baker et al., 1982). The main drawbacks in using TDR are that there are limitations regarding the depths to which it can be installed and that it only provides point source measurements. Researchers have also used dielectric sensors to estimate the liquid water content in frozen soils using a temperature dependent equation describing the permittivity of fresh water. For example, Sun et al., (2012) characterized freeze/thaw cycles using a dielectric sensor and illustrated the frost dynamics by transforming the measured liquid water content of frozen soil into different expressions, including frozen soil profile, frost penetration map, and freezing front trace. GPR can also be used to locate ground ice, the position of thermal interfaces and characterize the spatial variations of water content in the active layer (Moorman et al., 2003; Kneisel, et al., 2008). An example of GPR being used in permafrost areas is Yoshikawa and Hinzman, (2003), wherein GPR was used to study the draining of thermo-karst ponds. This study was able to utilize the boundary delineating properties of GPR to identify the role that permafrost plays in affecting the surface water balances.

Many permafrost areas are inhabited and thus require infrastructure such as housing and roads to support the local populace. If the permafrost in these areas begins to degrade (thaw), it can result in land subsidence which, in turn, poses a significant hazard to the surrounding infrastructure. Thus, permafrost monitoring of these areas has become a great concern (Nelson et al., 2001). GPR is a tool that is widely used to monitor permafrost degradation by identifying problematic areas (Moorman, 1994; Harris et al., 2001; Laxton and Coates, 2011). GPR has also been used in large scale monitoring projects such as The Norman Wells Pipeline project in order to delineate thermal transitions (Moorman et al., 2003). Mapping of frozen and thawed zones becomes very important within the context of permafrost degradation as discussed earlier. By using GPR Moorman et al., (2003) was able to identify areas of future permafrost degradation, areas where permafrost thaw had already taken place and the depth of thaw and frozen/unfrozen interfaces. Other applications of GPR in cryotic soils include: characterizing the occurrence of massive ice (Dallimore and Davis, 1992; Robinson et al., 1992; Wolfe, 1998), monitoring and identifying problem areas in frozen dam and ice roads (LaFleche et al., 1988) and measuring changes and developments to the depth of active layer thicknesses.

Recent advances in geophysical methodologies by Steelman and Endres, (2009); van der Kruk et al., 2009; Steelman et al., (2009); and Steelman et al., (2010), have shown that high-frequency ground penetrating radar (GPR) measurements can be used to non-invasively characterize highly dynamic shallow freeze-thaw processes. To the best of the author's knowledge, these latter studies are the first to use GPR to study shallow seasonal freezing and thawing in temperate regions. The outcomes from these latter studies indicate that GPR can provide high resolution, spatial and temporal characterization of seasonal freeze-thaw events.

As stated earlier, pore water freezing can alter soil structure, resulting in changes to the local hydrology of the area. If the soil is saturated, freezing conditions will cause the water to expand which will distort the pore voids and change the overall bulk density and structure of the soil (Unger, 1991). As a consequence of these changes, water flow through the frozen pores is impeded, thereby lowering the soil's permeability (Chamberlain and Gow, 1979). This decrease in permeability varies over space, leaving areas where water can infiltrate faster in some regions than in others. This spatially varied permeability distribution can lead to either depression focused infiltration of snowmelt or runoff at different locations in a catchment. How water infiltrates into frozen soil is a much debated process. In general, cryotic infiltration processes are lumped into one of three different categories; via restricted flow, limited flow, and unlimited flow (Gray et al., 1985). Restricted flow constitutes the presence of an ice lens on the surface or within the shallow soil and inhibits infiltration (Gray et al., 1985). Limited flow, allows for some snowmelt to pass through the soil and infiltrate into the ground (Gray et al., 1985). Limited flow depends upon many different factors and predicting the amount of limited flow and its occurrence is a great challenge for hydrologists (Woo et al., 2000). Outlined in point form are the most widely accepted limited flow theories:

- It has been recently reported that due to a relatively thin frozen layer, snowmelt infiltration was not impeded, compared to observations made in previous years with larger annual frozen layer maxima (Hirota et al., 2006; Iwata at al., 2008a). These observations suggest infiltration into a frozen layer may be due to the frozen zone thickness.
- Luo et al., (2003) suggests runoff is soley linked to water content and the influence of frozen soils on infiltration is weak.

- Zhao et al., (1997) suggests frozen soil infiltration has two primary regimes consisting of higher and lower infiltration rates controlled by thermodynamic processes.
- Sartz, (1969) reports changes in soil water takes place throughout much of the frost season, even with deep soil frost and observes water infiltrate and percolate through more than 60 cm of hard frozen ground.

The last infiltration regime allows for unlimited flow through frozen soils. This regime only occurs in soils containing large air-filled pores (e.g., macropores and fractures) (Gray et al., 1985). Freeze/thaw models simulate the infiltration into frozen soils; however, because the underlying processes are not fully understood by scientists, model developers are challenged to replicate field conditions through these models. Model developers have taken several approaches to overcome the absence of a governing equation that can describe this processes fully. Zhang et al., (2010) developed a simple parametric algorithm to describe infiltration into frozen soils that depends upon the initial water content, soil temperature and average surface saturation. Other approaches range from using empirical and semi/empirical observations to drive models, to attempting to fully couple mass, water, heat transport and phase change to predict infiltration on a more physical basis (ie., Zhang et al., 2008, SHAW, Flerchinger and Saxon, 1989; HYDRUS 1-D Hansson et al., 200). The minimal difference between observed and simulation infiltration rates are usually obtained through site specific calibration which can be costly and time consuming. The more physically based models usually have poor representation of soil moisture. These numerical models often have difficulty computing the highly non-linear behaviour resulting from the complex interrelationships of temperature, water and ice contents. Despite these shortcomings, models developed based on the most consistent theoretical understanding of these physical processes usually have the least amount of simplifying assumptions such as HYDRUS 1-D (Hansson et al., 2004; Ireson et al., 2013).

The groundwater regime in seasonally frozen regions of the world exhibits distinct behaviours (Williams and van Everdingen, 1973; Ireson et al., 2013). These behaviours generally are connected to the hydrologic processes of the area and water redistribution (Woo et al., 2000; Iwata et al., 2010). As noted earlier, the presence of ice in soil pores can change the permeability of a soil and thus influence the recharge and baseflow of local groundwater systems (Ireson et al., 2013). A decrease in the soil permeability results in less water reaching the watertable. This

situation is commonly observed during the winter when the ground is frozen and ice occupies the soil pores. Another phenomenon associated with freeze thaw cycles is depression focused infiltration, which has become a topic of interest to hydrogeologists because recharge of snowmelt can happen non-uniformly. This concept of non-uniform infiltration is a departure from what is usually observed in undisturbed soils where infiltration tends to be more evenly distributed across the landscape (Ireson et al., 2013). A relatively recent observation made by Iwata et al., (2010), suggests surface forces can cause a significant amount of groundwater to be redistributed upwards to the frozen zone. This suction is caused by a pressure differential and can impact groundwater storage during the winter. The decline in storage is temporary as the groundwater will be released from the frozen zone and be returned to the watertable during spring thaw. Despite this process only being temporary, it is still important for groundwater management programs as water redistribution and recharge is confounded by the unknown relative proportions of net infiltration versus vertical redistribution of moisture (Ireson et al., 2013).

The action of inhibiting long-wave radiation from leaving the Earth by way of CO_2 and/or CH_4 is the main driving force for climate change (Rosenzweig et al., 2008; Solomon, et al., 2007). Any changes to long-wave radiation will have notable effects to freeze/thaw cycles as ground thawing is in part, initiated by an increase in ground heat flux (Zhao et al., 2004). Moreover, freeze/thaw cycles are intimately connected to a plethora of hydrological processes and fundamental resources, thus any changes to freeze/thaw cycles can have unforeseen consequences; hence, more research on this topic is necessary. Predicting ground temperature is a key component to calculating ground heat flux and understanding climate change impacts better. In terms of accurately predicting soil temperature, knowing the extent of the frozen zone is very important. Small errors in soil temperature can yield very large errors in upward long-wave radiation calculations (Iwata et al., 2010). The prediction of the ground temperature is quite far from reliable; currently there is a lot of variability linked to differences in frozen soil schemes in models. For instance, models with an explicit frozen soil scheme give a more realistic depiction of soil temperature compared to those that do not. Luo et al., (2003) found that models that do not have a frozen soil scheme tend to have a 3 to 5 times larger amplitude of variation in temperature than what is observed in the field. Microbial productivity has been suggested to be a positive feedback for climate change as the breakdown of organic material by microbes can

release CO_2 and CH_4 to the atmosphere (Heimann and Reichstein, 2008). When soils are frozen, microbial productivity is inhibited; thus, less CO_2 is released and the feedback is broken for the duration the soils remains frozen (Henry, 2007). Therefore, the amount of time soils remain frozen can have important consequences for annual soil carbon and nutrient budgets. Changes to snow depth cover can also impact freeze/thaw cycles as snow has an insulating effect on the ground and can provide a muted response to winter temperatures and result in shallower depths of freezing and thus shorter overall freezing periods (Solomon et al., 2007). Solomon et al., (2007) observed changes to snow depth and cover and linked these changes to the effects of climate change. This aspect of climate change has important repercussions for the maximum depths and the total length of time soils remain frozen. Impacts to the agricultural industry have already been observed as a result to changes in snow pack depths. Hirota et al., (2006) highlighted the need for frost depth engineering in Northern Japan due to dramatic reduction in soil frost depths and the impact this reduction had on potato crops in the area. Freezing temperatures can act as herbicides and kill unwanted crops from previous growing seasons and restrict the need to manually pick out weeds which can be very time consuming and costly. This impact to the agricultural industry in Northern Japan was unexpected and emphasises the need for more research into the climate change and the impact to freeze/thaw cycles.

1.2 **Objectives**

The main objective of this thesis is to examine the capacity of surface GPR for quantitatively characterizing highly dynamic freeze/thaw processes. This thesis has been organized in a journal paper format where Chapter 2 represents that paper. To achieve this objective, a long-term winter monitoring campaign was employed using high frequency GPR. The winter campaign was executed by Steelman, (2012) and this work is based on data collected during that study. Steelman, (2012) utilized different survey methods (i.e., common-midpoint soundings and reflection profiles) to monitor and characterize subsurface processes. Steelman, (2012) conducted their surveys in an agricultural field located near Waterloo, Ontario over two winter periods, November 2006 - April 2007 and November 2007-April 2008. This study period captures a wide range of hydrological conditions that occur during the course of the winter season.

Using the Steelman GPR data set, the specific tasks performed in this study to achieve the main objective included:

- Use the high frequency GPR data set to characterize the freeze-thaw processes that occur during the two winter periods. This characterization consists of estimating the depth to the base of the frozen zone (BFZ) using the reflection event from this interface and inferring the presence of surface thawing through the occurrence of dispersive waveguide phenomena.

  Perform a numerical simulation of the freeze-thaw processes for the two winters with the HYDRUS-1D hydrological model with the available information for hydrological parameters and weather data for the Waterloo site. A model calibration for the 2007-2008 winter using a limited subset of the BFZ depths estimates from the GPR data will be done to determine the value of thermal properties for which there is no prior information
- Compare the results of the numerical modeling with the GPR monitoring results for the two winters.

1.3 Contributions to Research and Development

Portions of this thesis have been presented at regional, national and international conferences. A list of abstract presentations, including all collaborative authors, is provided below:

1. Anthony L. Endres, Alicia Beynon, Jennifer Hansen, Cameron W. Toy and Colby M. Steelman. Time lapse hydrogeophysical monitoring of near surface processes over long time periods. American Geophysical Union International Fall Meeting, 9th – 13th December 2012, San Francisco, USA.
2. Jennifer Hansen, Jon Paul Jones, Colby Steelman, Tony Endres. Monitoring winter processes using Ground Penetrating Radar. International Association of Hydrogeologist Annual Meeting, 16th-24th September 2012, Niagra Falls, Canada.
3. Jennifer Hansen, Jon Paul Jones, Colby Steelman, Tony Endres. (2012) Seasonal shallow freeze/thaw monitoring using Ground Penetrating Radar. Canadian Association of Geographer Annual Meeting, 28th May – 2nd June 2012, Waterloo, Ontario.

1.4 Tables and Figures

Table 1.1: A list of probes, instrumentation and methodologies currently used to measure frozen ground processes. Accuracy ranges are presented in degrees Celsius or meters. (Krzewinski et al., 1985)

Instrumentation		±	Unit
Ground Thermometry			
	Glass Thermometers	0.3 to 0.1	°C
	Bimetal Dial Thermometers	0.3 to 0.1	°C
	Frost Tubes	0.035	m
	Linear Resistance Thermometers	0.1	°C
	Themocouples	0.1 to 0.5	°C
	Thermistors	0.05 to 0.2	°C
Auguring/drilling		-	m
TDR		0.03	m

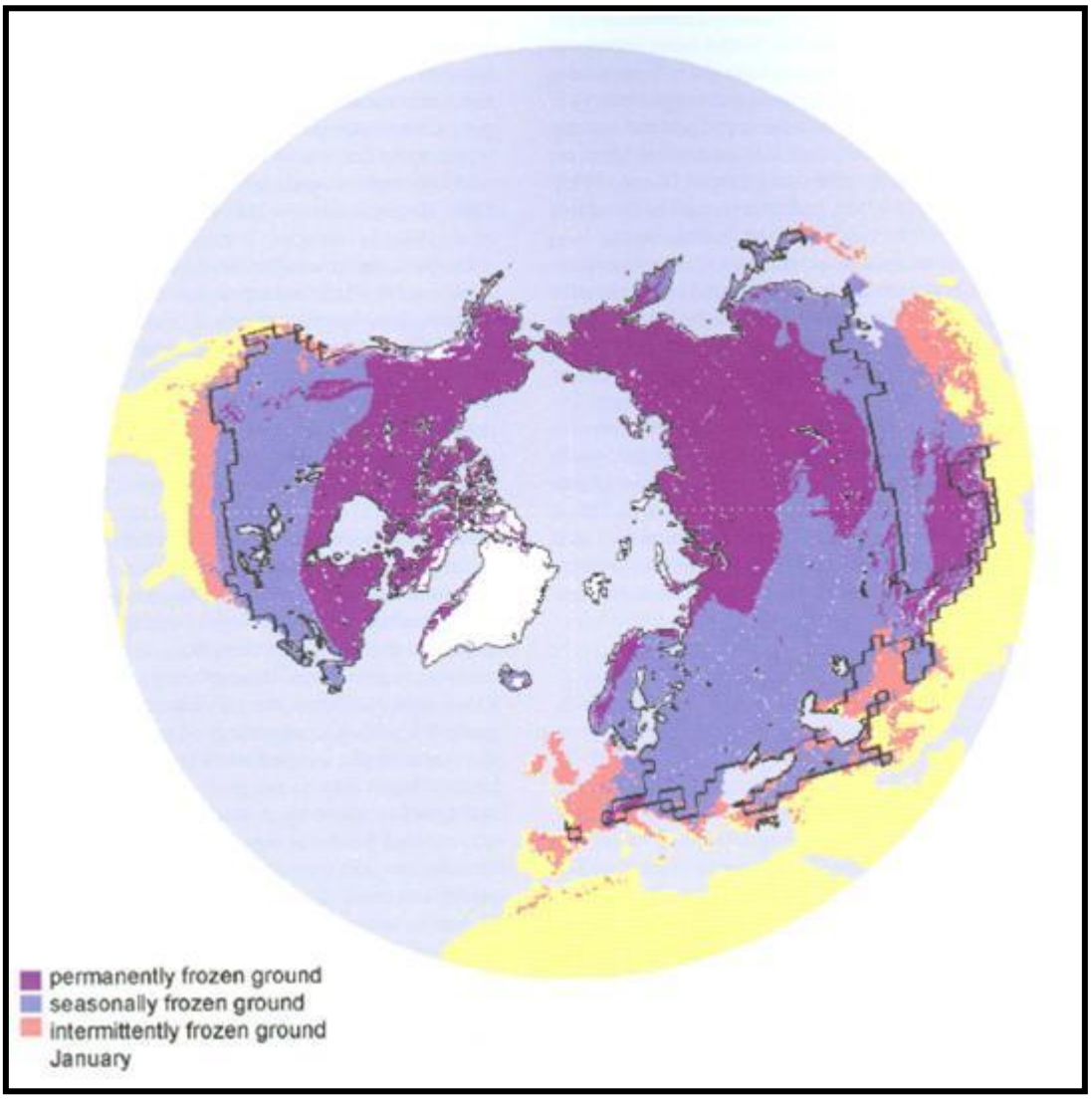

Figure 1.1 Distribution of permafrost, average maximum extent of seasonally and intermittently frozen ground (1950-1996) and average maximum snow cover extent (solid line, 1972-1995), in the Northern Hemisphere [from (Duguay et al., 2005) (Zhang et al., 2003)].

Chapter 2: Comparison of the Ground Penetrating Radar Monitoring of Winter Processes with HYDRUS-1D Modeling Results

2.1 Introduction

The inability to monitor seasonally frozen processes in northern latitudes has been identified as a major challenge in cold regions research (Woo et al., 2000; Iwata et al., 2010; Ireson et al., 2013). There is a significant need for the development of an effective method for measuring the unfrozen soil water content under frozen field conditions, and combining well-designed field experiments with modeling studies. Obtaining reliable and continuous data about the frozen state of the soil is a soil characteristic that has eluded researches but is continuously sought after because of its practical applications. For instance, joining knowledge from field studies with model development can expand the conceptual understanding of wintertime macroscale hydrological processes and help identify major gaps in the performance of numerical models simulating winter processes (Woo et al., 2000). Moreover, understanding the bigger picture of freeze/thaw cycles has large implications for groundwater storage, runoff and snowmelt infiltration as well as surface energy budgets (Luo et al., 2003).

At present, there is little agreement regarding the limiting and driving factors of snow melt infiltration and runoff into frozen soils. This disparity may be attributed to the limitation of the instrumentations and methodologies currently used for studying freeze thaw processes. The resolution of what these techniques can measure is not at the appropriate scale to capture all the intricacies and dynamic changes that are occurring during freezing and thawing cycles (Ireson et al., 2013). In seasonally frozen northern latitudes, the melting of snow in the spring is one of the most important hydrological events of the year, and is not completely understood (Zhao et al., 1997). This lack of understanding is, at least in part, due to the fact that the process of infiltration is not a simple switching mechanism, where permeable unfrozen soils converts to impermeable frozen soils, when a temperature threshold is crossed (Woo et al., 2000). As a consequence of this knowledge gap several competing theories regarding the driving mechanisms and controls on cryogenic soils infiltration have been developed. (Ireson et al., 2013). Here are a few examples of these competing theories:

- It has been recently reported that due to a relatively thin frozen layer, snowmelt infiltration was not impeded, compared to observations made in previous years with larger annual frozen layer maxima (Hirota et al., 2006; Iwata at al., 2008a). These observations suggest infiltration into a frozen layer may be due to the frozen zone thickness.
- Luo et al., (2003) suggests runoff is soley linked to water content and the infuence of frozen soils on infiltration is weak.
- Zhao et al., (1997) suggests frozen soil infiltration has two primary regimes consisting of higher and lower infiltration rates controlled by thermodynamic processes.
- Sartz, (1969) reports changes in soil water takes place throughout much of the frost season, even with deep soil frost and observes water infiltrate and percolate through more than 60 cm of hard frozen ground.

Other inconsistencies regarding the hydrologic community's general understanding of freeze/thaw processes are readily found in the literature. Henry, (2007) associates these inconsistencies to methodological differences between freeze/thaw studies and suggests the disparities diminish the relevance of many naturally occurring freeze/thaw cycles. For example, many laboratory freeze/thaw experiments do not adhere to an agreed upon representative minimum soil volume that can properly replicate natural field conditions (Henry, 2007). This lack of convention has led to overestimates of the impact ambient air temperatures have to exposed soil (Henry, 2007). To further illustrate, Grogan et al., (2001) reported temperature cycles of -7 and 10°C observed within soil cores of 21-24 cm in diameter and 12- 17cm deep, which were subjected to air temperature cycles of -15 and 20°C.

A greater understanding of the mechanisms driving wintertime processes is especially necessary with the uncertainly that climate change can bring to northern latitudes. In terms of areal extent seasonally frozen ground is the largest of the cryosphere components, having a long-term maximum areal extent of about 48 $x10^6$ km^2 (51%) of the land area in the northern hemisphere (Solomon et al., 2007). Thus, there is a motivation for understanding these freeze/thaw processes to better predict what is likely to happen under new climate regimes (Ireson et al., 2013).

At present, current studies investigating frost thawing may use one of five different methods that report a range of freezing and thawing soil effects (Henry, 2007). Moreover, conventional methods are invasive, point source techniques (e.g., frost tubes, glass and bimetal thermometers, thermisters) that may require numerous horizontally and vertically positioned probes at many depths. Invasive methods also tend to be unsuitable for large-scale investigations due to their higher costs and inability to ascertain the true subsurface characteristics due to their intrusive and indiscreet method of measurement. Understanding large scale processes is central to a complete understanding of freeze/thaw processes, because processes that are important at one scale may be negligible at another (Woo et al., 2000).

Recent hydrogeophysical studies (ie., Steelman and Endres, 2009; van der Kruk et al., 2009; Steelman et al., 2010), have shown that high-frequency ground penetrating radar (GPR) imaging can be used to non-invasively characterize highly dynamic freeze-thaw processes. This technique allows for high resolution, spatial and temporal characterization of seasonal freeze-thaw events, which can vary greatly during the course of a temperate winter season. Moreover, high-frequency GPR can capture the spatial heterogeneity and distribution of cryotic soils and provide valuable information to improve numerical heat transport and flow models to more accurately represent freeze/thaw cycles.

This study builds on the findings of these earlier works and enhances them by comparing the GPR characterization of the freeze-thaw processes with the results of numerical simulations of those processes. The simulations are performed using the HYDRUS 1-D model as modified by Hansson et al., (2004). These model is based on current understanding of freeze/thaw physics and while having limiting simplifying assumptions is considered to be one of the most sophisticated theoretical modeling packages for these processes (Ireson et al., 2013).

2.2 Site Information

2.2.1 Field Site

The GPR data used in this study were collected as part of the PhD dissertation by Dr. Colby Steelman (Steelman, 2012). These data were acquired at a site (43°29’4.85”N, 80°38’34.80”W) within an active agricultural field located on the Waterloo Moraine located 3 km west of Waterloo, Ontario, Canada. Details about this site are given in Steelman, (2012) and Steelman et

al., (2012) and are summarized here. The experimental site is positioned atop a local sand hill characterized by interbedded fine to coarse sand to an approximate depth of 10 m. The presence of these stratified clean sands resulted in excellent depth penetration and high resolution GPR imaging.

2.2.2 Winter Weather Conditions

Meteorological data used in this thesis were obtained from the University of Waterloo weather station located approximately 7 km east of the site. Figure 2.1 and Figure 2.2 shows the daily high and low temperatures and cumulative daily precipitation for the period from mid-October to mid-April for the winters of 2006/2007 and 2007/2008, respectively. These two winters provide a unique opportunity to examine the ability of high-frequency GPR imaging to characterize winter processes under significantly different seasonal conditions and compare those observations with modelling results.

Freezing conditions for the 2006/2007 winter had a later start compared to the average winter conditions with November, December and the first half of January being unseasonably warm. The second half of January 2007 brought colder, freezing temperatures followed by a very cold and dry February. February had only 27.4 mm of precipitation, which is considerably less than the long-term average of 51.3 mm for this month. These conditions resulted in a thin snow pack that would be expected to impact the depth of the frost front for the 2006/2007 winter. March 2007 brought the end of freezing conditions with the second half of the month being warm and wet.

During the 2007/2008 winter, freezing conditions commenced in late November and persisted through early January. A major intra-seasonal thaw event occurred during January 6^{th}-11^{th} with the record-breaking high temperature of 13.3 on January 8^{th} that was the fourth highest temperature observed in the Waterloo Region since records began in 1915. Further, approximately 50 mm of rainfall occurred during this event with 33.2 mm on January 9^{th}, making it the wettest January day since 1995. The weather in February 2008 was consistent with historical averages, with freezing temperatures and average amount of snow fall. March 2008, however, was colder than the average. A number of short warming and cooling cycles in February and March resulted in corresponding transient shallow freeze-thaw events with the main spring thaw occurring in early April. Overall, this winter was wetter than average (268.9

mm versus the long term average 189.0 mm) with a record breaking snowfall of 257.5 cm with the previous record of 245.3 cm occurring 1924.

2.3 Description of the Unsaturated Flow and Heat Transport Model

2.3.1. Variably Unsaturated Flow

The HYDRUS 1-D code used for this study, was modified by Hansson et al., (2004), this modified code has the capability to simulate freeze/thaw processes along with unsaturated flow. This version of HYDRUS 1-D was adopted for this study as it proved to be one of the most consistent theoretical models available for understanding the physical processes of vadose zone freeze/thaw cycles due to its minimum amount of simplifying assumptions (Ireson et al., 2013). HYDRUS 1-D version 4.15 simulates the one-dimensional movement of water and heat in variable-unsaturated media. This software numerically solves a modified version of the Richards equation for variably unsaturated flow and heat transport solutions. Equation 1 describes the flow portion of the numerical solution for above and below zero temperatures (e.g., Fayer, (2000), Noborio et al., (1996a.))

$$\frac{\partial \theta_u(h)}{\partial t} + \frac{\rho_i}{\rho_w}\frac{\partial \theta_i(T)}{\partial t} =$$

$$\frac{\partial}{\partial z}\left[K_{Lh}(h)\frac{\partial h}{\partial z} + K_{Lh}(h) + K_{LT}(h)\frac{\partial T}{\partial z} + K_{vh}(\theta)\frac{\partial h}{\partial z} + K_{vT}(\theta)\frac{\partial T}{\partial z}\right] - S$$

Equation 1

where θ_u is the volumetric unfrozen water content (L^3L^{-3}) which, is distributed between the volumetric vapour water content and volumetric liquid water content ($\theta_u = \theta + \theta_v$). The quantity θ_v is expressed as a volumetric water content equivalent (L^3L^{-3}). The other variables ρ_i, ρ_w, h, T, t, and θ_i represent the density of ice (ML^{-3}), density of liquid water (ML^{-3}), pressure head (L), temperature (K), time (T) and volumetric ice content (L^3L^{-3}) respectively. The spatial coordinate z is positive upward. A sink term S accounts for the uptake of water through plant roots. For Equation 1, the subscripts u, i, w, Lh, LT, vh, and vT denote unfrozen water, ice, liquid water, liquid flow, temperature gradient, vapour flow due to pressure head and temperature, respectively.

Equation 1 solves the unsaturated flow regime by breaking down the flow system into different processes. This equation represents five processes that all have their own corresponding hydraulic conductivity value. The first three terms on the right hand side represent the flow of liquid water through porous media. The first term describes the flow of water due to a hydraulic gradient, the second term describes gravity flow and the third term incorporates flow due to a temperature gradient. The last two terms solve the vapour transport portion of the flow system, for gradient and temperature induced flow respectively.

Equation 1 is highly non-linear and often leads to numerical instabilities with the combination of HYDRUS 1-D solving the heat transport and vapour transport portion of the code. Therefore, the vapour transport portion of the code was left inactive for this study. Justification for turning off this process was based on the fact that soil medium of the study a medium to coarse grained sand and vapour transport in an unsaturated large pore medium is much less compared to that in silt or clays (Ireson et al., 2013; Hoekstra, 1969; Dirksen and Miller, 1966). In essence, this assumption presumes that the vertical downward flow of water is the dominant form of water movement and vapour transport is negligible.

The study considered the use of both the Brooks and Corey, (1964) and van Genuchten, (1980) relationships to describe the capillary pressure-water saturation properties of the study site. The Brooks and Corey relationship originally was our choice to represent the hydraulic characteristics because it generated better fitting curves to the laboratory data when compared to the van Genuchten curve. Further, Steelman et al., (2012) obtained good fits between GPR observations and modeling prediction when using the Brooks-Corey relationship to simulate the behaviour of this system for unfrozen conditions. However, when attempting to simulate frozen conditions using HYDRUS 1-D, the model had convergence difficulties that were very likely due to the discontinuity in the Brooks and Corey curve. To overcome these convergence problems, the original Brooks and Corey, (1964) curves were replaced with corresponding van Genuchten curves which made the model more numerically stable.

2.3.2. Heat Transport

HYDRUS 1-D modified by Hansson et al., (2004) considers the transport of heat by conduction as well as convection with flowing water. Heat transport in a variably unsaturated porous medium is described as (e.g., Nassar and Horton, 1992):

$$\frac{\partial C_p T}{\partial t} - L_f \rho_i \frac{\partial \theta_i}{\partial t} = \frac{\partial}{\partial z}\left[\lambda(\theta)\frac{\partial T}{\partial z}\right] - C_w \frac{\partial q_l T}{\partial z} - C_w S T$$

Equation 2

The first term on the left hand side of the equation represents changes in energy for the system, where C_p represents the volumetric heat capacity of the porous media [$ML^{-}T^{-2}K^{-}$]. The second term represents the latent heat of the frozen phases. The terms on the right hand side of the equation represent soil heat flow by conduction and transfer of sensible heat through movement of water respectively. The parameter C_w is defined by volumetric heat capacity of liquid water [$ML^{-}T^{-2}K^{-}$]. The last term in the equation represents the uptake of energy associated with root water uptake. The parameters $\lambda(\theta)$, L_f, and ρ_i, represents the latent heat of freezing [$L^{-}T^{2}$], thermal conductivity [$MLT^{-3}K^{-}$] and the density of ice [ML^{-3}] respectively. The subscripts for Equation 2, p, f, l denote porous media, freezing, and flowing water respectively.

The volumetric heat capacity (C_p) is the sum of the product of the solid (C) and the volumetric heat capacity of the solid (n), water (w), organic matter (o) and air phases (a). C_p is defined as the sum of all the phases multiplied by their respective volumetric fractions θ or a in the case of the gas phase.

$$C_p = C_n\theta_n + C_w\theta + C_o\theta_o + C_a a_v$$

Equation 3

L_f in Equation 4 denotes the latent heat of freezing [$L^{-}T^{-2}$] which is approximately 3.34 x 10^5 J kg^{-}. C_p is redefined as apparent volumetric heat capacity C_a; this value takes in to account the increase in heat capacity when the freezing point is reached (Carsel and Parrish, 1988). Equation 4 defines C_a [$ML^{-}T^{-2}$].

$$C_a = C_p - L_f \rho_i \frac{d\theta_i}{dT}$$

Equation 4

The parameter $\lambda_o(\theta)$ represents the thermal conductivity, which describes the transmission of heat through the porous medium and water, but does not take into account the flow of water or macrodispersivity. Equation 5 describes this process (Campbell, 1985).

$$\lambda_o(\theta) = A + B\theta - (A - D)\exp[-(C\theta)^e]$$

$$A = \frac{0.57 + 1.73\theta_q + 0.93\theta_m}{1 - 0.74\theta_q - 0.49\theta_m} - 2.8\theta n(1 - \theta n)$$

$$B = 2.8\theta_n$$

$$C = 1 + 2.6\theta_c^{-\frac{1}{2}}$$

$$D = 0.03 + 0.7\theta_n^2$$

e=4

Equation 5

where subscripts q, m, n, and c denote the volumetric fractions of quartz, other minerals, total solid grains and clay particles, respectively in the study. Estimates of quartz and the amount of other mineral volumetric fractions were performed through optical grain analysis from samples collected directly from the field. Table 2.1 lists the measured quantities for these parameters including clay and total solid grain fractions. To incorporate the difference in conductance between ice and water, Equation 6 was modified by Hansson et al., (2004) to more accurately represent processes at sub-zero temperatures. They allowed for the ice fraction to contribute to the thermal conductivity which can make a significant difference for relatively low temperature when the liquid water content is small and the ice content is relatively high. Equation 6 incorporates these changes and by replacing θ, with $\theta+F\theta_i$, where F is given by:

$$F = 1 + F_1\theta_i^{F2}$$

So that $\lambda_o(\theta) = A + B(\theta + F\theta_i) - (A - D)\exp[-(C(\theta + F\theta_i)^e]$

$$\lambda(\theta) = \lambda_o(\theta) + \beta_t C_w|q_w|$$

Equation 6

The apparent thermal conductivity takes into account longitudinal diffusivity (β_t) and flow, which is described in Equation 6.

2.4 Field Data and Analysis

2.4.1. Soil Characterization

Pitting and coring was done at the study site by Steelman, (2012) to determine the soil hydraulic properties and obtain information about the subsurface stratigraphy. Details about this sampling and the subsequent laboratory tests are found in Steelman, (2012) and Steelman et al., (2012). For this study, the water retention curves were generated from the data collected from Steelman's hanging water column experiments were fitted to a non-hysteretic van Genuchten relationship and used to estimate unsaturated conductivity parameters. This relationship expressed in as a function of pressure head (h) is defined as follows in Equation 7:

$$\theta(h) = \begin{cases} \theta_r + \dfrac{\theta_s - \theta_r}{[1 + |\alpha h|^n]^{1/n}} & h < 0 \\ \theta_s & h \geq 0 \end{cases}$$

$$K(h) = k_s S_e^l [1 - (1 - S_e^{\mathrm{n}})^{1/n}]^2$$

$$S_e = \frac{\theta - \theta_r}{\theta_s - \theta_r}$$

Equation 7

The above equations contain five independent parameters: θ_r, θ_s, k_s, n, and α, which describe residual water content, saturated water content, saturated hydraulic conductivity respectively; and the last two parameters are empirical quantities. The pore-connectivity parameter l in the hydraulic conductivity function Equation 7 was estimated to be about 0.8 as an average for sandy soils (Mualem and Dagan, 1977). Equation 7 is the expression for effective saturation, corresponding to the total water content θ.

Table 2.2 gives a summary of the hydraulic property values used in the HYDRUS 1-D modelling in this study obtained from the direct sampling and lab experiments conducted by Steelman. The hydraulic parameters are mostly homogeneous with 2 distinct layers. The top portion of the soil column from 0 to 0.25 m represents the plough zone and has lower hydraulic conductivity, higher porosity and residual saturation compared to the rest of the soil medium. The portion below this zone was assumed hydraulically homogeneous.

2.4.2. GPR Data and Processing

The GPR data used in this thesis were acquired were collected as part of the PhD dissertation by Dr. Colby Steelman (Steelman, 2012) that examined the capability of GPR to monitor and characterize near-surface hydrological processes over two complete annual cycles from August 2006 to October 2008. The GPR data for each field date consist of a coincident common midpoint sounding (CMP) and reflection profile these data pairs were obtained along a fixed 10 meter survey line at intervals a daily to weekly basis. During the first 10 months, the reflection profiling covered the middle 2 meters of the survey line (i.e., 4.00-6.00 meter station positions); afterwards, the coverage of the reflection profiling was extended to the middle 8 meters (i.e., 1.00-9.00 meter station positions). The CMP soundings were located at the center of the reflection profiles (i.e., 5.00 meter station position).

A Sensors and Software PulseEKKO™ 1000 (Sensors and Software Inc., Mississauga, Ontario, Canada) GPR system equipped with 900 MHz antennas was utilized to acquire GPR data. A time window of 100ns, sampling interval of 0.1 ns and 64 stacks per trace was used. The reflection profiling was performed with a constant antenna offset distance of 0.17 m (using manufacturer's brackets) and a station increment of 0.02 m. The CMP data was acquired using a 0.02 m separation increment and a minimum offset of 0.20 m. The maximum offset for the CMP sounding varied between 2.00 to 6.00 m; larger offsets were used to characterize dispersive wavefields when they were present. Data was processed using Reflex-Win™ software program (Sandmeier Software, Karlsruhe, Germany). The processing steps are summarizing in Table 2.3 for reflection profiles and CMP soundings.

2.4.3. Identification of the Base of the Frozen Zone (BFZ) from Reflection Profiles

Reflection profiles were used to initially identify the reflection event generated by the frozen/unfrozen interface at the base of the frozen zone (i.e., BFZ event). This event can be observed on the profiles when BFZ has progress to sufficient depth such that its reflection is not obscured by the high amplitude early time arrivals (i.e., the direct air and ground waves). When this condition is satisfied, the BFZ event is generally observed as a laterally continuous reflection extending across the entire profile; it is superimposed over the reflection events corresponding to stratigraphic boundaries. The BFZ event differs from the stratigraphic reflections in two important attributes.

First, the BFZ reflection is an ephemeral event; it is only present during the winter period when the observed EM wave velocities, such as the DGW velocities, indicate the frozen ground conditions. Conversely, the stratigraphic reflections are persistent events that are readily identifiable throughout the complete annual cycle. This feature is illustrated in Figure 2.3 where the BFZ event is clearly present during frozen conditions (February 14, 2008), but is absent during unfrozen conditions in immediately preceding (November 1, 2007) and after (April 10, 2008) the winter period.

In addition, it was commonly observed that the reflectivity of the stratigraphic boundaries was significantly decreased when subjected to freezing conditions (i.e., interfaces located above the BFZ event on the reflection profiles) compared to their reflectivity during the unfrozen conditions before and afterwards. This phenomenon is exhibited in Figure 2.3 where the reflectivity of the shallow stratigraphy events on the February 14 profile is considerable reduced relative to their reflectivity of these events on the November 1 and April 10 profiles. The reduction in reflectivity is likely due to the changes the reflection coefficient resulting from the dielectric permittivity decreases that occur when liquid water (κ_w ~ 86) is transformed into ice (κ_i ~ 3.2).

Second, while the two-way traveltime of stratigraphic reflections vary with the in-situ conditions, their configuration relative to one another is always consistent due that these interfaces are fixed within the subsurface. In contrast, the BFZ event shifts vertically with respect to the stratigraphic reflections as the frozen conditions evolve. This behaviour is seen in Figure 2.4 where the BFZ event is observed to propagate downwards relative to the stratigraphic reflection during February 2008.

2.4.4. GPR Estimates of the BFZ Depth

Estimates of the BFZ depth were obtained from the CMP sounding data using normal moveout (NMO) analysis of its reflection event. NMO analysis is a commonly used technique for deriving velocity-depth information from the two-way traveltime-antennae offset distance relationship of reflection events. This analysis is based on the hyperbolic representation to the traveltime-antennae offset distance relationship given by

$$[t_x]^2 = [t_0]^2 + x^2/[V_{NMO}]^2$$

Equation 8

where the velocity V_{NMO} and zero offset t_0 define the best fitting hyperbola to the traveltime-offset distance data.

The BFZ and stratigraphic reflection events were identified at the short offset distances on each CMP sounding by visually correlation with the corresponding reflection profile. The semblance plot generated in NMO analysis component of the Reflex-Win™ software program was used to identify the hyperbolic traveltime-offset distance relationship of the BFZ event to the larger offset distances on the CMP sounding. Figure 2.5 shows an example of this procedure where the marked BFZ event on the CMP sounding correlates with the BFZ event and major semblance peak. Further, the value of the V_{NMO} velocity (0.156 m/ns) corresponding to semblance peak is consistent with the range of EM wave velocities for frozen soil at this site.

After the BFZ event was identified on the CMP sounding data, its traveltime-offset distance data were obtained using the event picking procedure in Reflex-Win™. To maintain consistency in the picking process, the trough of BFZ event was used. These traveltime-offset distance data were analyzed using the x^2-t^2 method to determine V_{NMO} and t_0 of the best fitting hyperbola defined by Equation 8. The use of the x^2-t^2 method allowed us to estimate the uncertainties in the V_{NMO} and t_0 values (e.g., Jacob and Hermance, 2004).

The results of the x^2-t^2 method were subsequently used to determine the BFZ depth z_{BFZ} using the following equation

$$z_{BFZ} = V_{NMO}\, t_0 \,/2$$

Equation 9

as well as an estimate its uncertainty. These values are complied in Table 2.4 . Dates when the high quality GPR data allowed the unambiguous identification of the BFZ event on both the reflection profile and CMP sounding are indicated in bold type. Depth values from these dates were used to calibrate the HYDRUS 1D model.

2.4.5. Occurrence of Thawed Layer Waveguides

The thawing of the shallow part of the frozen ground during mid-season freeze-thaw cycles produces low velocity surface layer overlying the frozen soil that act as a waveguide. While the

thawed layer is generally too thin to be properly resolved by either reflection profiling or CMP soundings, the effects of this waveguide can be clearly seen in both the profiling and sounding data. For the CMP soundings, the waveguide produces a dispersive wavefield that immediately follows the direct ground wave (DGW) event (van der Kruk et al., 2009). The thawing process results in small-scale heterogeneities that produce in near-surface scattering that appears as steeply inclined wavefields on the reflection profiles (Steelman et al., 2010). These wavefields are also dispersive because they propagate in the thawed waveguide. An example of both of these thawed waveguide effects is illustrated in Figure 2.6. The dates on which these dispersive thawed waveguide phenomena were observed in the GPR data are listed in Table 2.5. The timing of these events were compared with predicted occurrence of thawing by HYDRUS 1-D.

2.5 Modelling methodology

2.5.1. Model Set Up

The system being considered in this work is relatively simple from a hydrologic perspective. In terms of the conceptual model, frost heaving, vapour flow, evapotranspiration, macropore flow and hysteresis are ignored and a simplified conceptual hydraulic model very similar to the one described in Steelman et al. (2012) was used. A customized version of HYDRUS 1-D code with enhanced freeze-thaw simulation capabilities was used for this study (Hansson et al., 2004). This customized version of the code was chosen for this work because it has a minimal number of simplifying assumptions and, therefore, is one of the most consistent theoretical models currently available for understanding the physical processes of vadose zone freeze/thaw cycles (Ireson et al., 2013).

Most of the values for the soil hydraulic properties used by Steelman et al., (2012) which are based on their laboratory measurements and sampling were used as input parameters for HYDRUS 1-D to simulate unsaturated vertical flow in this system. However, their use of the Brooks and Corey, (1964) soil-water characteristic curve led to numerical instabilities occurring when portions of the system became fully saturated during the simulation of winter processes. To avoid these problems, the van Genuchten, (1980) soil-water characteristic curves to represent the capillary pressure-saturation relationships in this study. Figure 2.7 shows the van Genuchten, (1980) soil-water characteristic curves and the laboratory measured capillary pressure-saturation data for the two soils types used in the simulations; the value of the van Genuchten parameters

are given in Table 2.2. It can be seen that there is good fit between them for the range of effective saturations below 0.85. The relatively lower air entry pressure values specified by van Genuchten curves were necessary to avoid numerical instabilities.

The heat transport portion of the code was either driven by parameters based on the field sampling or standard values derived from the literature. These are listed in Table 2.6 with the literature values denoted with an asterisk. For this study, the value of the solid phase heat capacity parameter was determined by model calibration with the GPR data (this process is described below) and is also listed in Table 2.6**.**

Boundary conditions for the model were based on site conditions. A free drainage boundary condition was set at the base of the profile (10 m.b.g.s.) which allowed soil moisture to drain vertically across the lower boundary. This boundary condition was considered the best choice because the water table is well below the zone of interest and is expected to have no significant effect on the soil profile moisture dynamics (Steelman et al., 2012). The upper boundary condition was designed to simulate atmospheric conditions by adding a surface layer which computes fluid fluxes across the upper boundary driven by external conditions. This upper boundary condition subjects the soil-air interface to changing atmospheric conditions such as temperature and precipitation. However, HYDRUS 1-D takes into account the actual moisture conditions near the surface when computing fluxes; therefore, there are two different types of fluxes, actual and potential.

Precipitation during colder periods was also simulated as snow fall and its accumulation and melting was simulated by the model. HYDRUS 1-D assumes that all precipitation falling during temperatures below -2°C is snow and +2°C is rain with a linear mixing between the two in the -2°C to +2°C range. If a snow pack exists and temperatures are above zero, then the melting constant is used to calculate melting rates.

2.5.2. Model Calibration

The HYDRUS 1-D model was calibrated by adjusting the thermal parameters to obtain the best fit between the model results and the good quality GPR estimates of BFZ depth given in Table 2.4. Before the calibration process began, a sensitivity analysis was carried out to identify potential model calibration parameters. Based on the results of this sensitivity analysis, it was

determined that the model predictions for simulated BFZ depths were quite sensitive to changes in the soil heat capacity parameter and less sensitive to changes in the other parameters. The soil heat capacity is the amount of energy required to raise the temperature of a gram of soil one degree Celsius.

The soil heat capacity is a storage term that significantly impacts to the overall depth of the BFZ in the modeling results while retaining its general temporal trend. An increase in the soil heat capacity parameter value in the model decreases the overall predicted BFZ depth generated for the season. Model calibration consisted of varying the soil heat capacity parameter in a logarithmic fashion over a range of plausible values while the other heat-related parameters remained fixed. The resulting root-mean-square error (RMSE) between the BFZ depth predictions obtained from HYDRUS 1-D and the corresponding depth estimate obtained from using only the good quality GPR data are given in Figure 2.8 where it can be seen that the best fit between the simulated and observed BFZ depths was achieved with a soil heat capacity of 3.34 Jg^{-1} $°K^{-1}$.

It should be noted that this calibration derived value for the soil heat capacity parameter (3.34 Jg^{-1} $°K^{-1}$) is somewhat higher than the commonly accepted range for this value such as one given by Chesworth, (2008) (i.e., 0.83-1.076 Jg^{-1} $°K^{-1}$). Its relatively high magnitude suggests that a larger soil heat capacity value was needed to compensate for the underestimation of water contents as HYDRUS 1-D creates an ice barrier that allows very little water to infiltrate downward during frozen conditions. As noted by Woo et al,. (2000) and Luo et al., (2003), this barrier assumption is physically incorrect which, in turn, means that the model will systematically underestimate water contents under frozen conditions.

2.6 Comparison Between GPR Observations and Simulated Winter Processes

A numerical simulation using HYDRUS-1D was done for the period from November 15, 2007 to April 15, 2008 (i.e., days 153) during which the occurrence of frozen soil conditions were observed at the study site. The simulation was programed to start from June 6, 2007 to allow for a spin-up period. Running the simulation for 6 months prior to frozen soil conditions gives the simulation enough time to reach an equilibrium state and depart from initial conditions. In total, the simulation was run for 325 days with a time step of 0.001 days (15 min). The representative

volume was set to residual saturation (-100 cm of pressure head) as an initial condition and a temperature of 20 °C. The results of this simulation are given Figure 2.9 where the frozen soil interval and the zone of near-surface thawing are both shown. This simulation indicates two main periods of frozen soil conditions (i.e., late November to early January and mid-January to early April) that are separated by the major intra-seasonal thaw event. In addition, there is a significant amount of shorter term fluctuations in the BFZ depth during each of these main periods. The simulation also predicts numerous short-term near-surface thawing events with the thaw zone depths ranging up to more than 0.20 meters.

The BFZ depth estimates obtained from the GPR data are compared with 2007-2008 simulation in Figure 2.9. It can be seen that there is good overall agreement between HYDRUS-1D predictions and the corresponding GPR estimates of the BFZ depth using both the high quality GPR data that was used for the model calibration and the lesser quality GPR data sets. This agreement is well displayed in Figure 2.10. The dates when the dispersive waveguide phenomena were observed in the GPR data are also indicated in Figure 2.9. These events correlate well with the episodes of surface thawing predicted by the HYDRUS-1D simulation. Further, the dispersive waveguide inversion procedure of van der Kruk et al., (2006) was applied to the CMP data from February 8 and April 2 by Steelman et al., (2010) and van der Kruk et al., (2009), respectively, to estimate the thawed zone thickness on each date. The thawed zone thickness estimates (0.06 m for February 8 and 0.15 m for April 2) compare well reasonably with the corresponding model predictions (0.3 m and 0.1 m for February 5 and 6 respectively and 0.13 m and 0.28 m for April 1 and 2 respectively).

A second numerical simulation using HYDRUS-1D was done for the period from November 15, 2006 to April 15, 2007 (i.e., days 153; the results of this simulation are given Figure 2.11. In contrast to the 2007-2008 simulation, the 2006-2007 results show a shorter period of the long-term frozen soil conditions from mid-January to late March with no significant thawing events before the end of seasonal frozen soil conditions. Further, there is very little short term fluctuations in the predicted BFZ depth during the 2006-2007 simulation.

The BFZ depth estimates obtained from the GPR data are compared with 2006-2007 simulation in Figure 2.10. While the GPR monitoring dates were significantly sparser than the 2007-2008

season, there is good overall agreement between HYDRUS-1D predictions and the corresponding GPR estimates of the BFZ depth for the available monitoring dates w9here the BFZ event could be imaged. In addition, van der Kruk et al., (2009) obtained a frozen soil thickness of 0.40 m on January 17, 2007 from the analysis of the dispersive wavefield due to the occurrence of a "leaky" waveguide (i.e., a thin, high velocity frozen layer overlying low velocity unfrozen wet soil). This value is comparable with the corresponding HYDRUS-1D modelling predicted thickness of the frozen zone (0.03 m) for January 17, 2007.

2.7 Discussion and Conclusions

This study represents the first attempt to examine in detail the capability of high frequency GPR to characterize seasonal freeze–thaw processes in a temperate climate. This objective was accomplished by comparing the results obtained from a multi-year GPR data set covering two contrasting sets of winter conditions with predictions from a version of HYDRUS-1D capable of simulate freeze/thaw processes along with unsaturated flow. In particular, estimates of the depth to the BFZ and the occurrence of surface thawing events were considered in this study.

While almost all of the parameters required for the numerical simulation were obtained from independent sources (e.g., laboratory measurements on samples from the study site), it was necessary to perform a model calibration to determine the value of soil heat capacity using a limited subset of the GPR estimates of the BFZ depth from the 2007-2008 winter season. It was noted during this calibration process that while the value of soil heat capacity significantly influenced the magnitude of the BFZ depth, there was significant less impact on the predicted timing of BFZ advances and recessions.

In general, there is good overall agreement between the HYDRUS-1D modeling predictions and the corresponding GPR estimates of the BFZ depth for both winter seasons used in this study. In addition, the occurrence of dispersive waveguide phenomena were observed in the GPR data match well with episodes of surface thawing predicted by the numerical simulation. These results strongly indicate that the surface GPR data used in this study gives reliable information about seasonal freeze-thaw processes. Further, this GPR-derived information has the potential to be used in the calibration of the numerical simulations of these processes.

The ability to image the reflection event corresponding with the BFZ boundary is an important element in the use of GPR data to characterize seasonal freeze-thaw processes. A factor that affects the imaging of this event is the magnitude of its reflectivity. During this study, it was noted that this event had higher reflectivity during periods when the BFZ was advancing downwards. During periods of upward recession, the reflectivity of BFZ event was greatly reduced and frequently could not be identified with confidence. It is possible that these reflectivity changes are the result of the different conditions occurring at this boundary during its advance and recession.

While the large dielectric permittivity contrast due the downward transition of the soil moisture from ice (κ_i ~ 3.2) to liquid water (κ_w ~ 86) has the potential to produce significantly high reflectivity for the BFZ event, the strength of this reflection is also dependent on the thickness of the region over which this transition happens. In principle, a thinner transition region would generate higher reflectivity for the BFZ event. Hence, the observed change in reflectivity could be an indication the transition from frozen to unfrozen conditions takes place over a thinner depth interval as the BFZ advances downwards in comparison to the interval thickness during BFZ recession upwards. Further work is necessary to explore this point.

2.8 Tables and Figures

Table 2.1 Volumetric fractions (L^3/L^{-3}) of soil components used in the volumetric heat capacity equation. These values are based on visual examination of samples from the site.

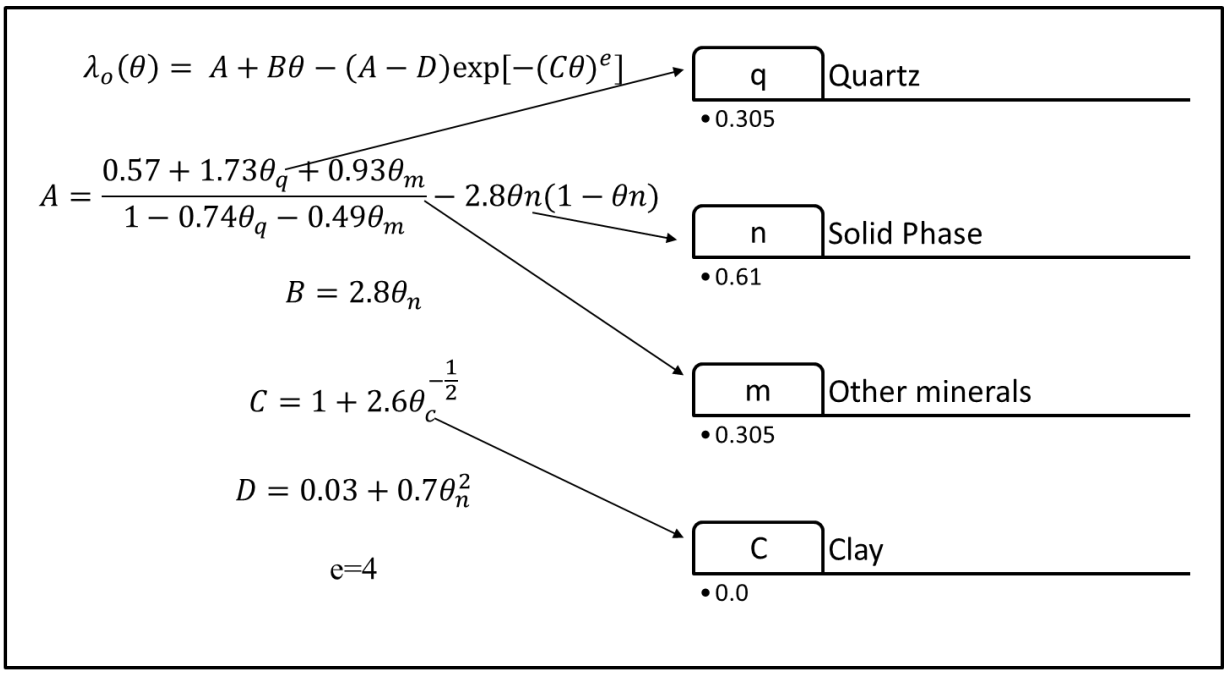

Table 2.2: Hydraulic properties for soils used in HYDRUS 1-D model.

Depth (m)	α (1/m)	n (-)	l (-)	θs (-)	θr (-)	K_{sat} (m/s)
0 - 0.25	2.8	2.12	0.8	0.39	0.071	1.3×10^{-4}
0.26 - 10	3	3.9	0.8	0.39	0.058	3.0×10^{-4}

Table 2.3: Lists the processing steps applied to raw GPR data after acquisition. An asterisk shown indicates that a given processing step was applied to a survey type.

GPR Processing steps	Common Midpoint Soundings	Reflection Profiles
Subtract-mean (dewow) Heat Capacity ($Jg^{-} K^{-}$) Time window= 1.11	*	*
Mean filter Mean range= 4	*	
Walsh bandpass Lower cutoff = 1 Upper cutoff = 1000		*
Time cut Uniform time window = 15 ns	*	*
Gain function Start time= 0.1 Linear gain [1/pulsewidth] =0.8 Exponent [db/m]=1000	*	*
Bandpass frequency Lower cutoff = 100, Lower plateau=200 Upper cutoff= 1100, Upper plateau= 1400	*	
Move start time	*	*
Zero time correction Using linear extrapolation to zero-offset (CMP)	*	

Table 2.4: A summary of the depth to base of frozen zone (BFZ) determined from the GPR data and predicted from the HYDRUS 1-D simulation. The estimated uncertainty of the GPR depths is given in the parentheses. Bold values represent high-quality GPR data sets used to calibrate the HYDRUS 1-D model.

Date	GPR 900 MHz (m)	HYDRUS 1-D (m)	Difference (m)
06-Dec-2007	0.36 (±0.01)	0.38	0.02
21-Jan-2008	0.44 (±0.01)	0.46	0.02
24-Jan-2008	0.51 (±0.01)	0.61	0.10
28-Jan-2008	0.73 (±0.01)	0.73	0.00
31-Jan-2008	0.75 (±0.07)	0.68	-0.07
11-Feb-2008	0.60 (±0.01)	0.53	-0.07
14-Feb-2008	0.60 (±0.01)	0.80	0.20
18-Feb-2008	0.73 (±0.01)	0.84	0.11
25-Feb-2008	0.91 (±0.01)	0.91	0.00
29-Feb-2008	0.92 (±0.02)	0.93	0.01
03-Mar-2008	0.97 (±0.04)	1.01	0.04
06-Mar-2008	0.98 (±0.02)	0.99	0.01
10-Mar-2008	0.92 (±0.03)	0.92	0.00

Table 2.5: A list of dates on which dispersive diffractions due to the thaw-induced near-surface waveguide occurred on the GPR refection profiles

Dispersive Wave Guide Dates
January 2008
07
08
February 2008
08
March 2008
03
17
18
19
21
28
30
April 2008
1
2

Table 2.6: Heat transport parameters for HYDRUS 1-D model. The brackets indicate the parameter whose value was altered during model calibration

Air	2.5
Water	4.18
[Solid phase]	[3.34]

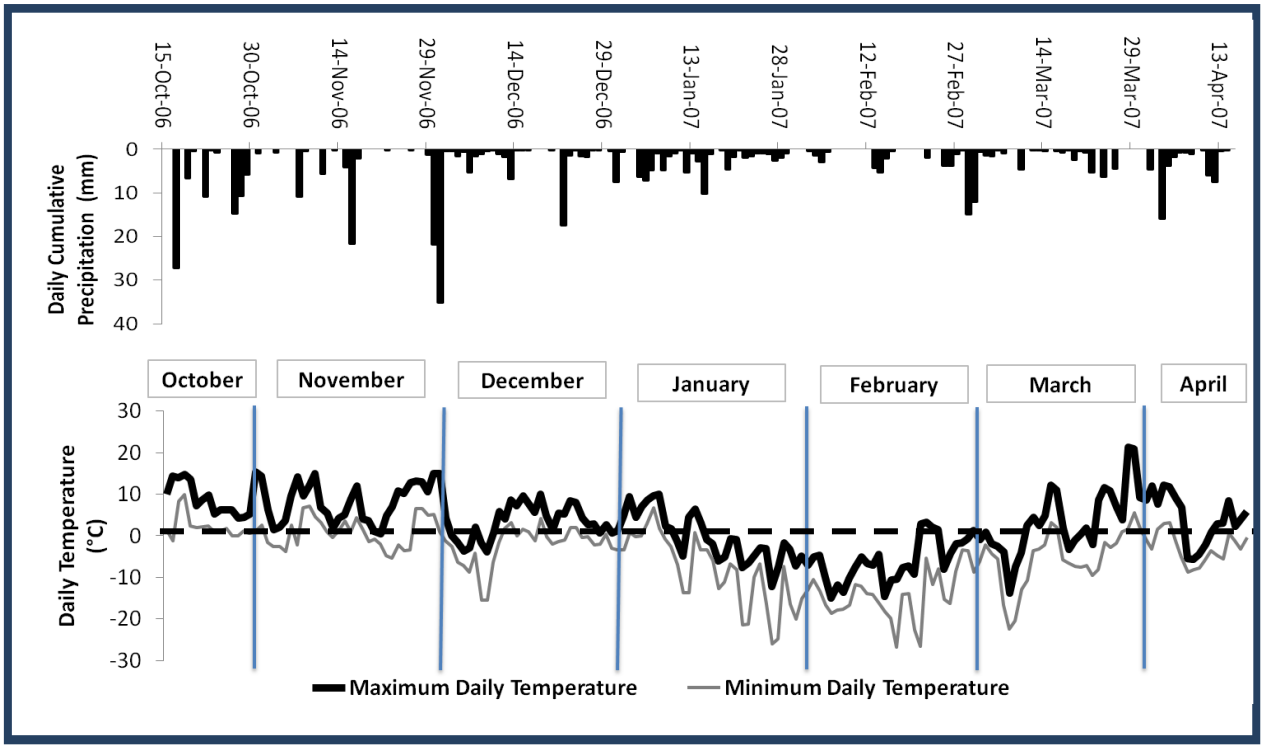

Figure 2.1: (Top) Daily cumulative precipitation in millimetres from October 15, 2006 till April 15, 2007. (Bottom) Plot showing the daily temperature highs and lows in degrees Celcius. The dotted line indicates 0 degree Celcius on the graph; freezing temperatures occur below the dotted line.

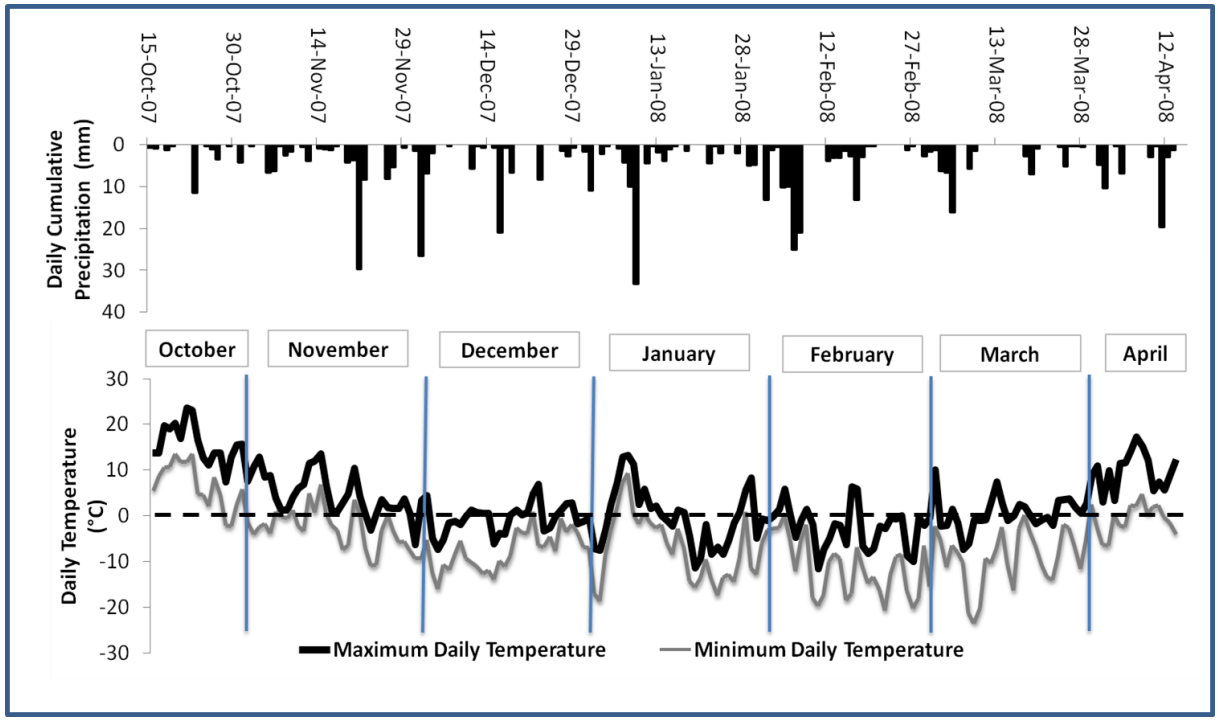

Figure 2.2: (Top) Daily cumulative precipitation in millimetres from October 15, 2007 till April 15, 2008. (Bottom) Plot showing the daily temperature highs and lows in degrees Celcius. The dotted line indicates 0 degree Celcius on the graph; freezing temperatures occur below the dotted line.

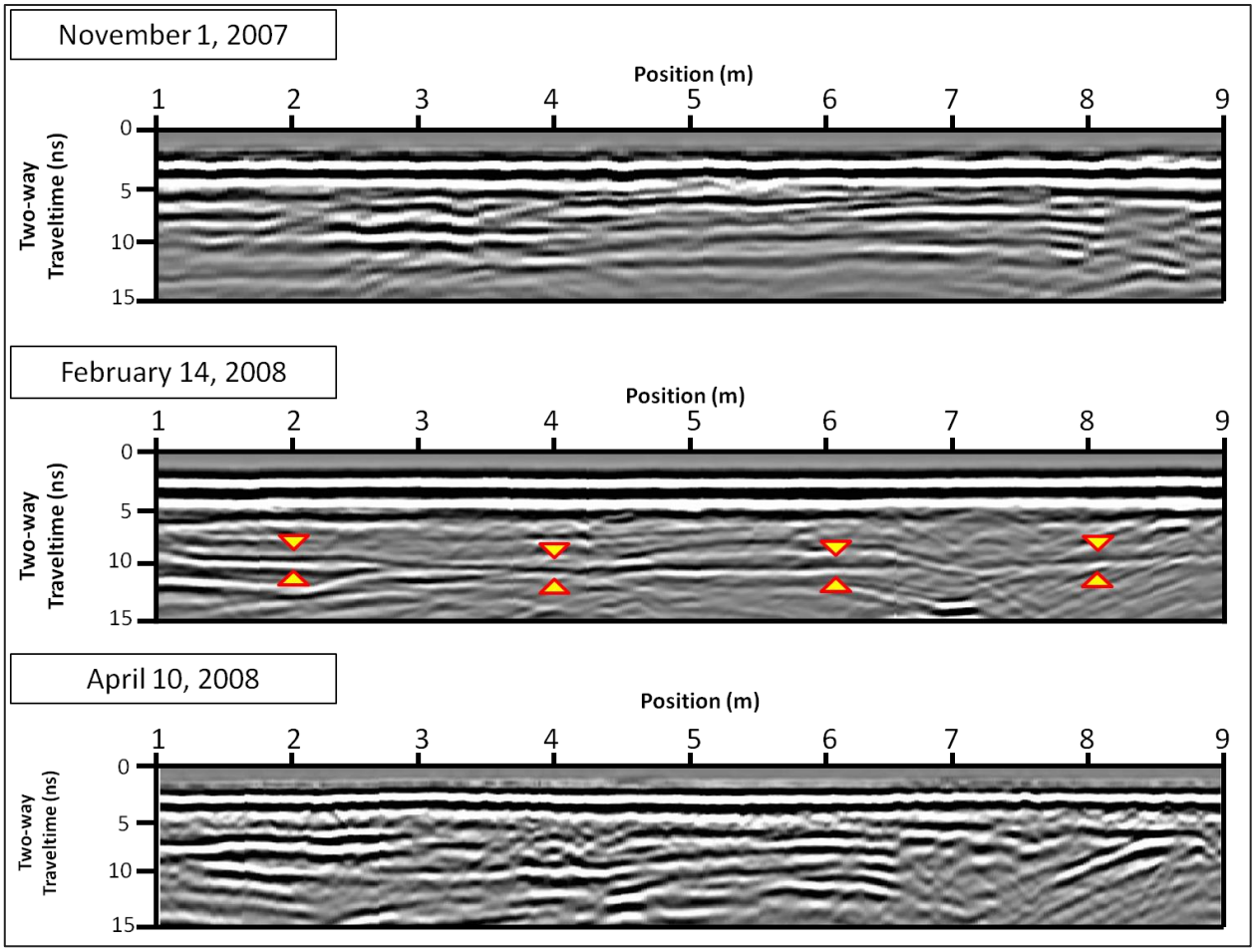

Figure 2.3: Selected GPR reflection profiles illustrating the differences in imaging between frozen winter conditions (February 14, 2008) and unfrozen conditions in the preceding late fall (November 1, 2007) and after in early spring (April 10, 2008). The winter profiling is characterized by the appearance of the BFZ reflection event; yellow arrows outlined in red denote the position of this ephemeral reflection. In addition, this winter data also display the reduced reflectivity of the stratigraphic reflection lying above the BFZ event that is commonly observed.

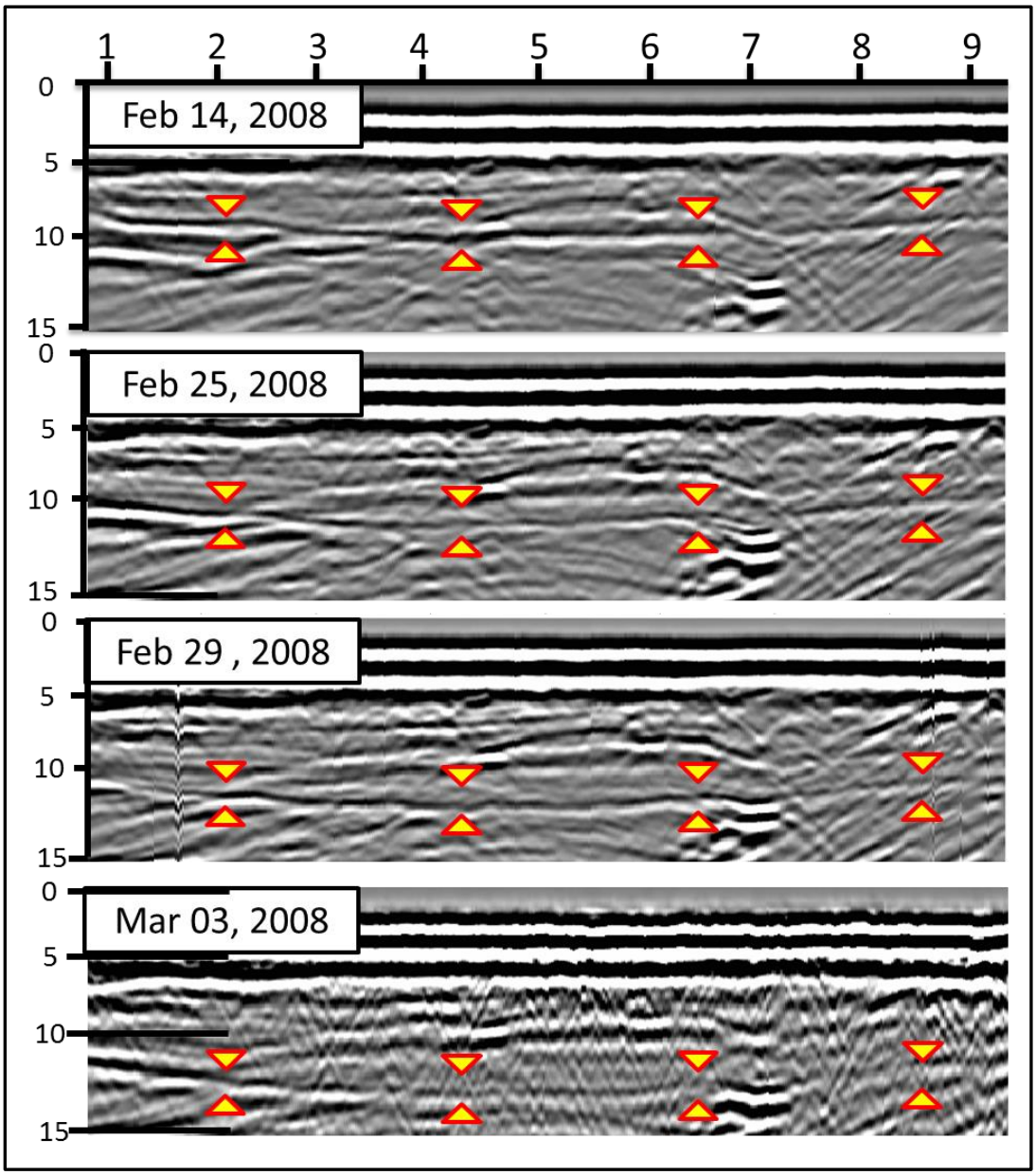

Figure 2.4: GPR reflection profiles imaging the downward advancement of the BFZ reflection event from February 14th 2008 till March 3, 2008. Yellow arrows outlined in red pin point the position of the frost front on the GPR images.

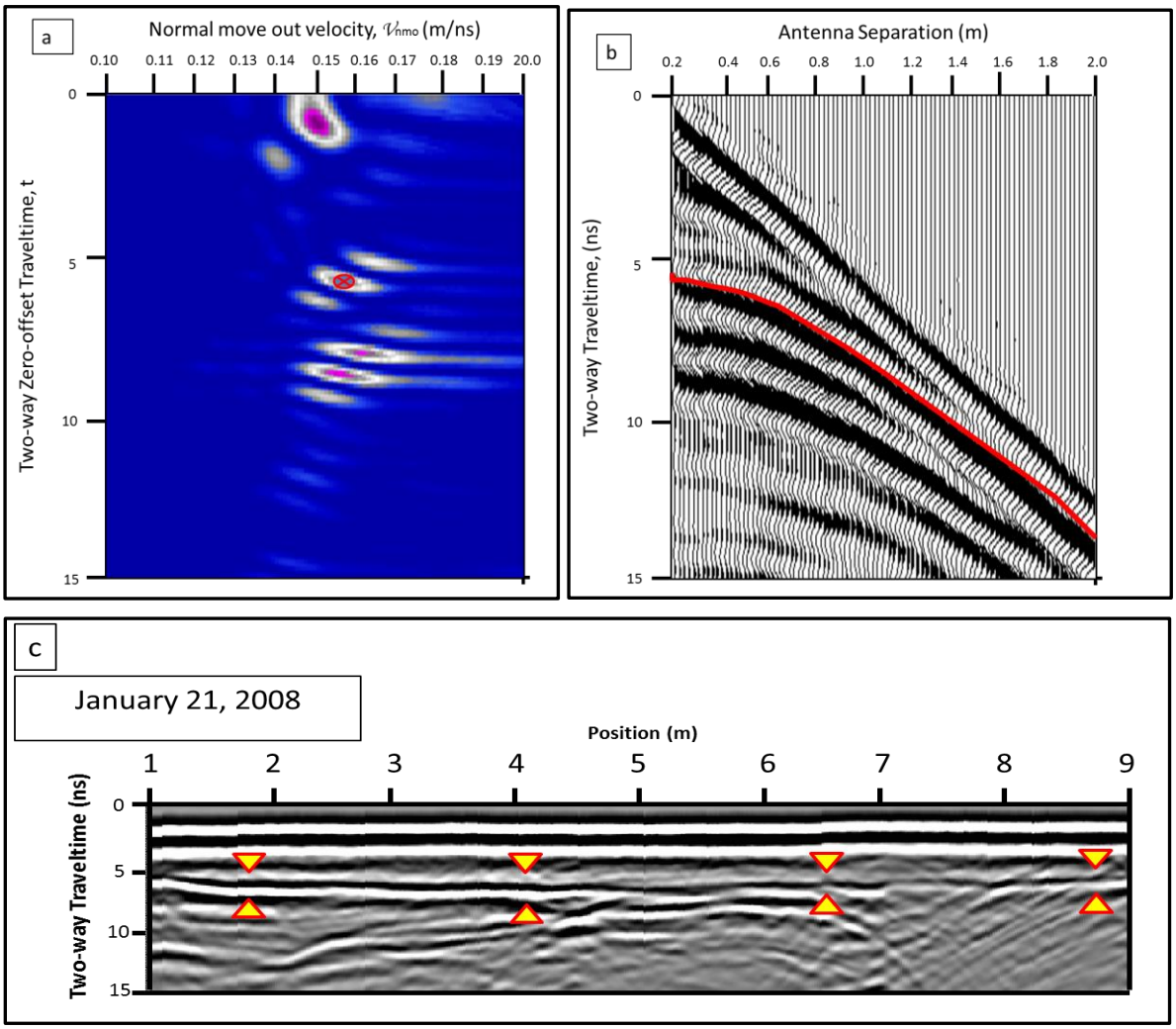

Figure 2.5: An example of the procedure for estimating the BFZ depth from GPR data. Identification of the BFZ reflection event on the reflection profile (a). Yellow arrows outlined in red indicate the position of this event. The corresponding CMP sounding (b) with the red hyperbola showing identified BFZ event that was used to obtain the traveltime-offset data. The semblance plot (c) generated from the CMP sounding that was used to select the BFZ event. Red x indicates the semblance peak corresponding to the hyperbola shown on the CMP sounding.

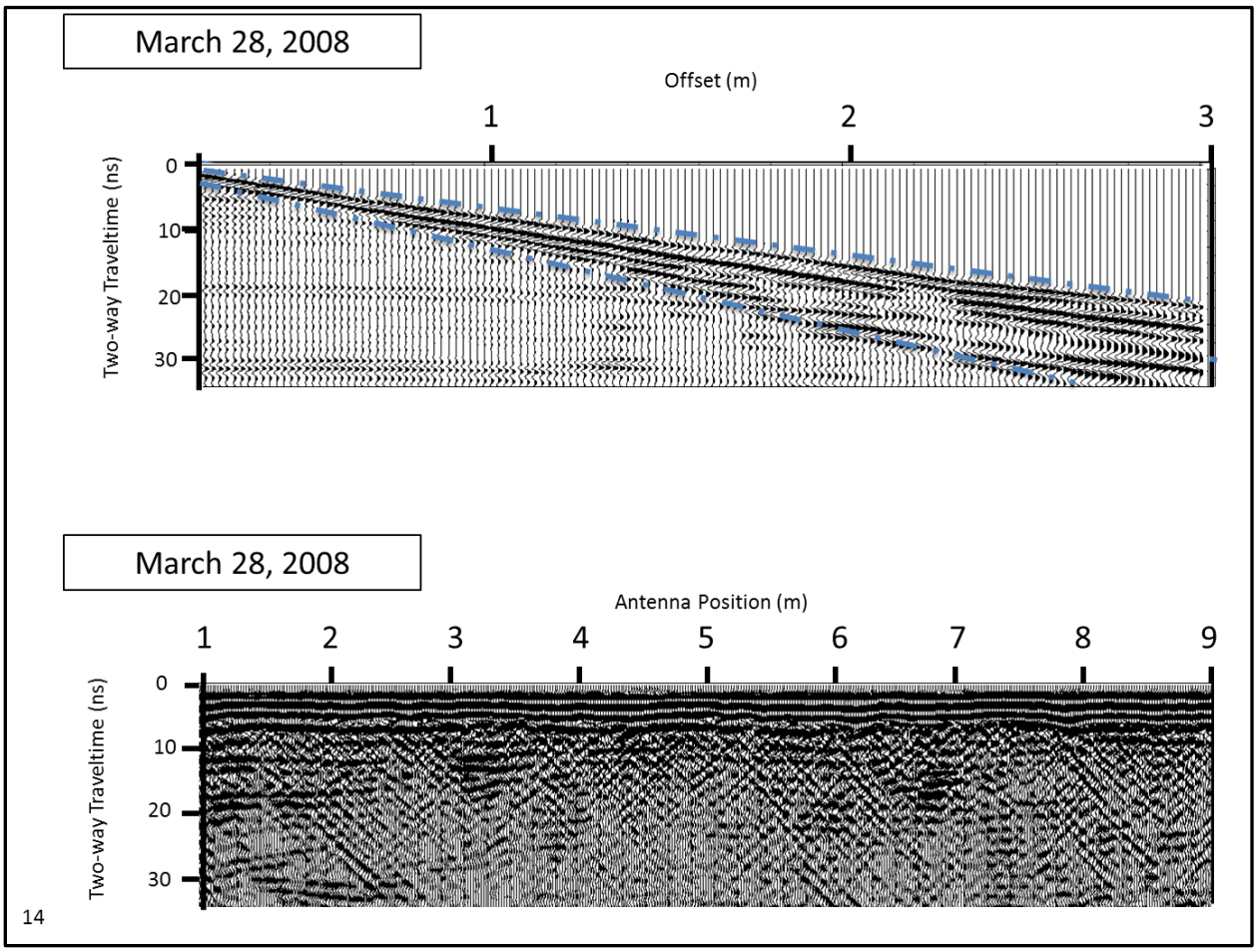

Figure 2.6: The impact of the near surface low velocity waveguide resulting from thawing on the CMP sounding (top) and reflection profile (bottom). Dashed blue line in CMP shows dispersive wavefield. The numerous dipping linear events on the reflection profile are dispersive diffractions due to small heterogeneities in the near surface waveguide that occur during thawing.

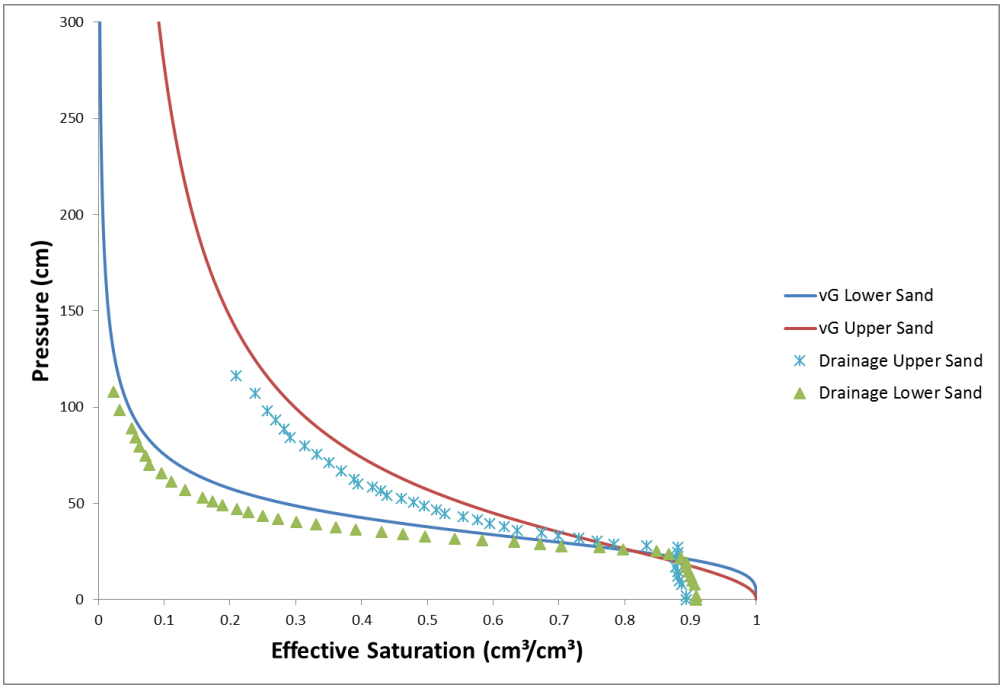

Figure 2.7: Comparison between the drainage curves and the van Genuchten-Mualem curves for the upper and lower sands for the Waterloo site. The van Genuchten-Mualem curves are slightly modified to reduce the air entry value to avoid numerical instabilities in HYDRUS-1D modeling.

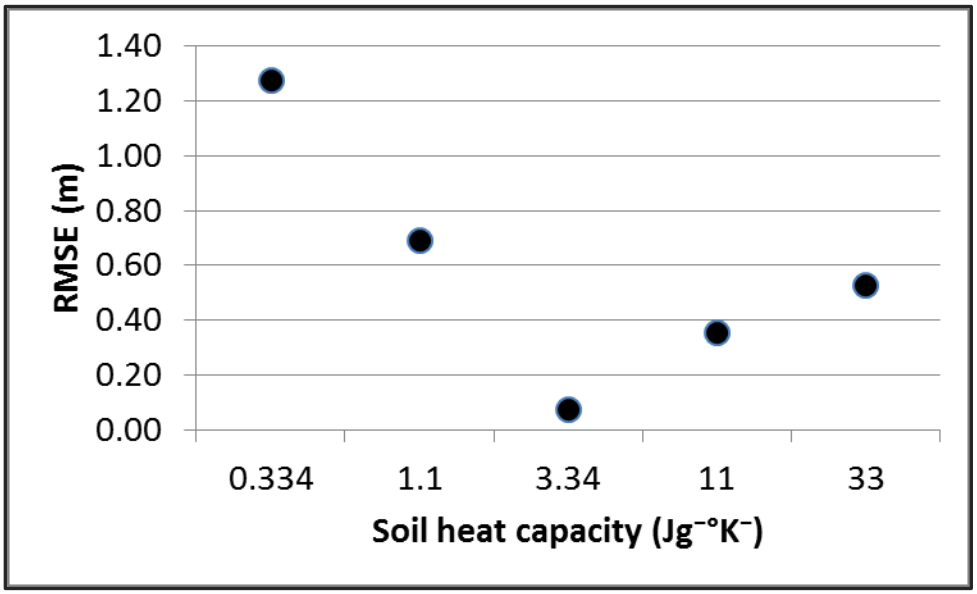

Figure 2.8: RMSE values obtained during HYDRUS-1D model calibration process as a function of soil heat capacity

Figure 2.9: Comparison between the results of the HYDRUS 1-D numerical simulation and observations for the GPR data (BFZ depth estimates and occurrence of dispersive near-surface diffraction events) for the 2007-2008 winter season. High quality BFZ depth estimates from GPR data used for HYDRUS-1D model calibration indicated by filled symbols. Uncertainty in BFZ depth estimates are shown by error bars.

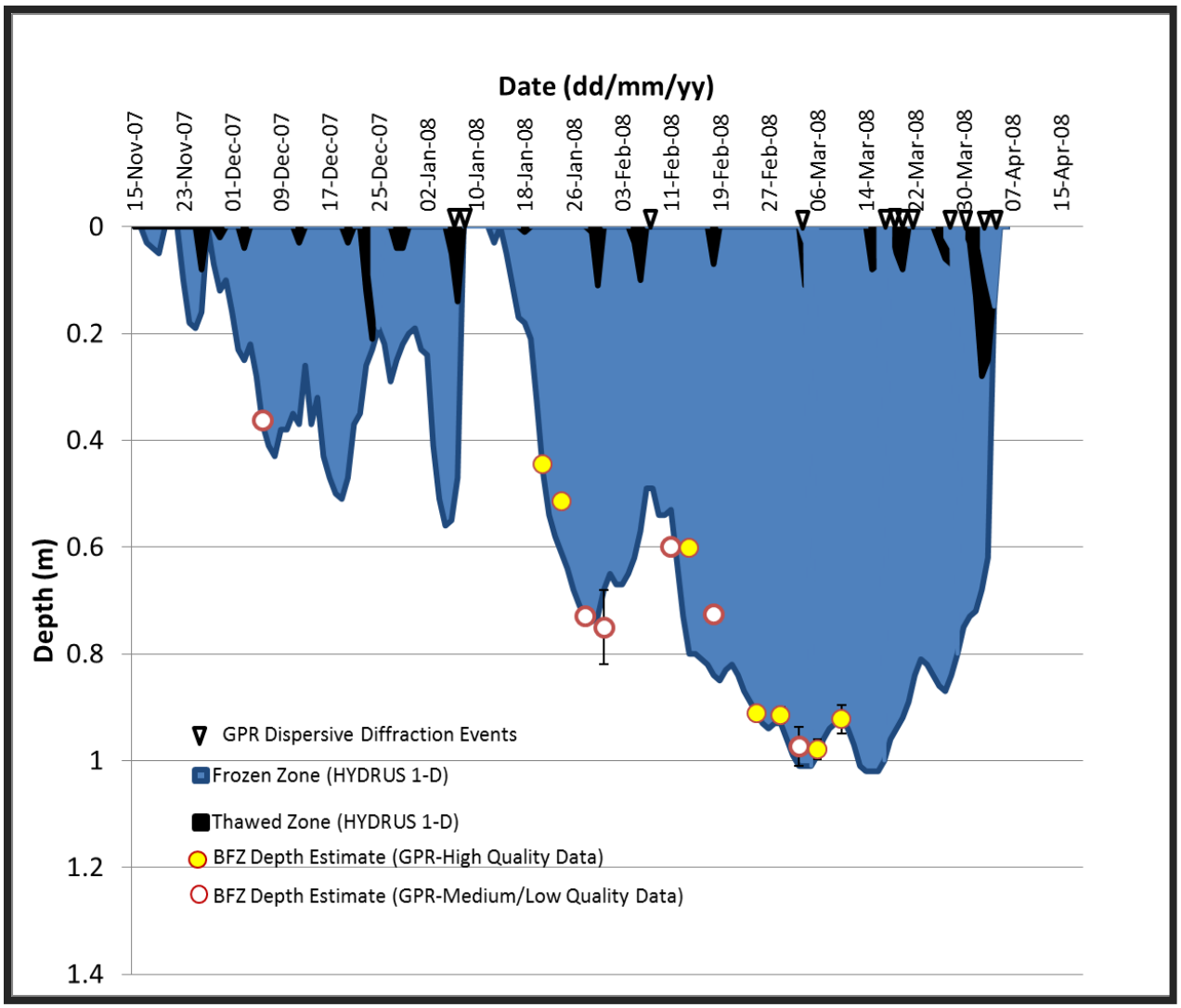

Figure 2.10: Comparison between the results of the HYDRUS 1-D numerical simulation and observations for the GPR data (BFZ depth estimates) for the 2006-2007 winter season. Uncertainty in BFZ depth estimates are shown by error bars.

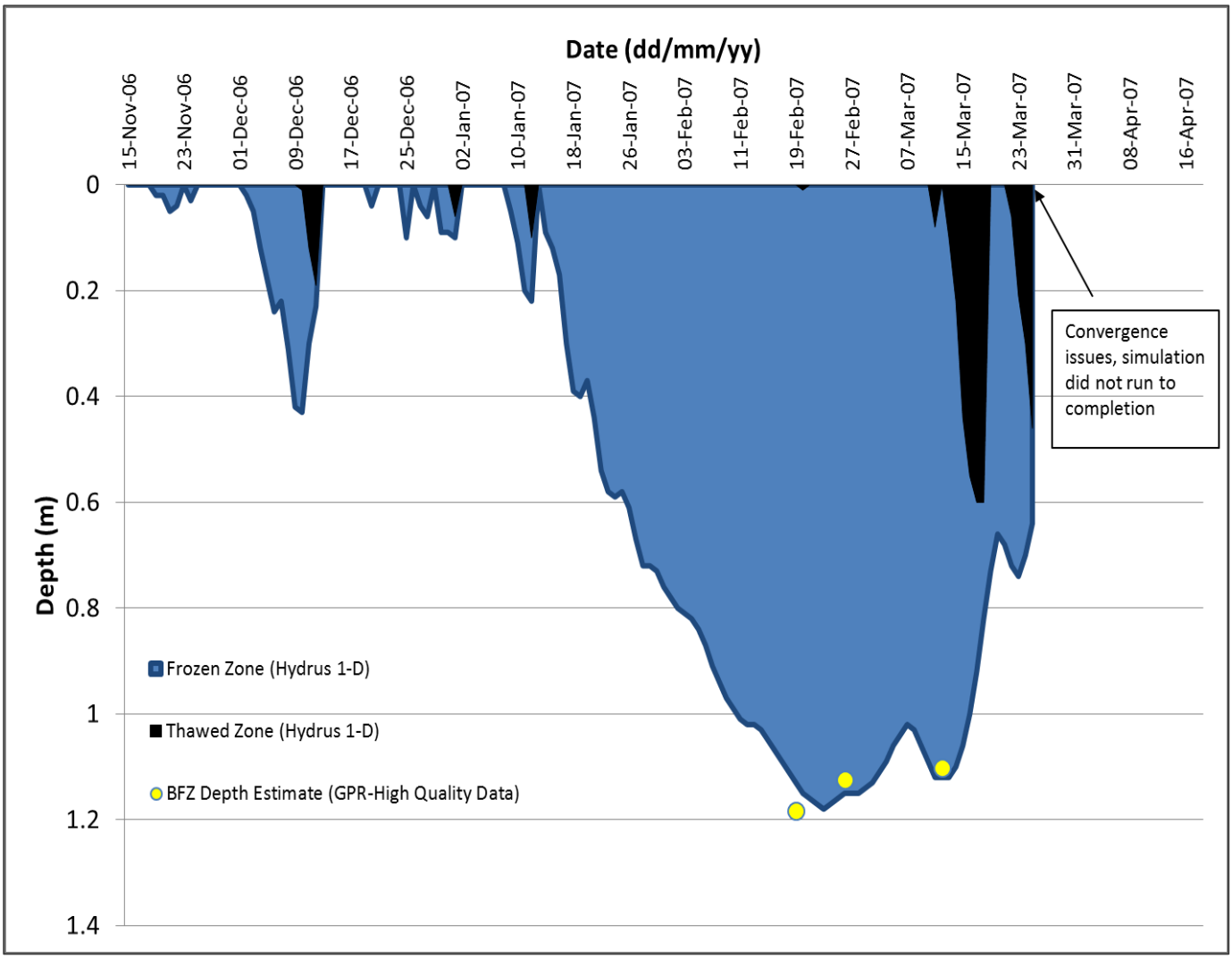

Figure 2.11: Cross plot showing the correlation between the BFZ depth estimates based on the HYDRUS 1-D modeling results and those obtained from GPR data for the 2007-2008 winter. The high quality GPR data used for model calibration are denoted by (SYMBOL); GPR estimates obtained from medium/low quality data sets are given by (SYMBOL). The solid line denotes equal values.

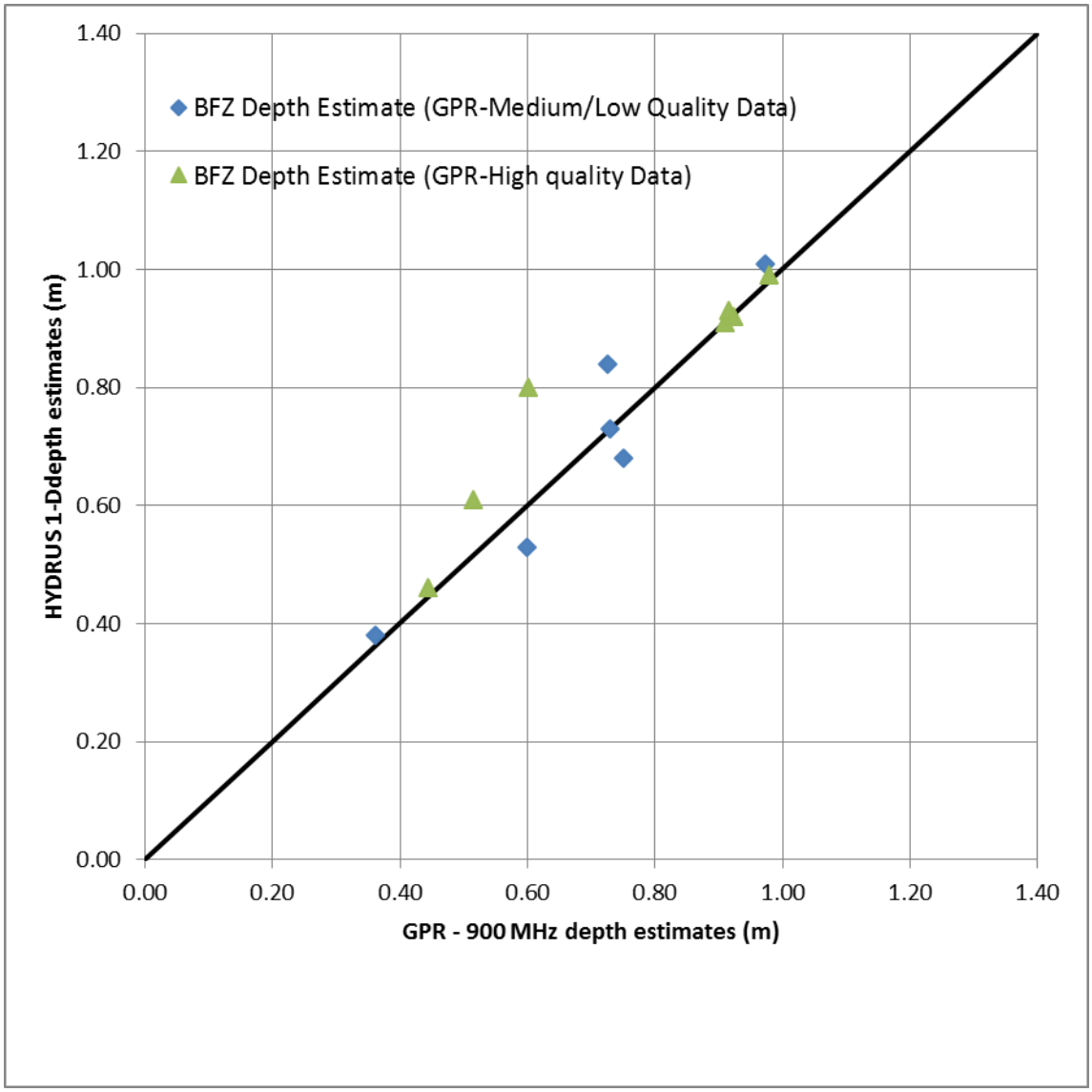

Chapter 3: Summary and Recommendations

3.1 Summary of Main Contributions

The goal of this thesis was to assess the capacity of surface GPR to characterize seasonal freeze/thaw processes. High frequency GPR can provide high resolution, spatial and temporal data about the frozen subsurface; this comprehensive new measurement strategy can capture aspects of freeze/thaw processes that have previously been below the detection limit of earlier instrumentations and methodologies. To perform this assessment, an analysis of high frequency (900 MHz) GPR data obtained by Steelman (2012) that provide detailed monitoring during two winter seasons was undertaken. This data set consisted coincident CMP soundings and reflection profiles for each monitoring date.. The GPR measurements were performed at intervals ranging from 1 day to 4 weeks over different periods between November 2006 and April 2008 and captured a range of soil conditions including small and large thawing events, a completely frozen condition and transitions between moisture ranges (Steelman et al 2012).

Obtaining a comprehensive understanding of freeze/thaw cycles and determining the influence it can have on hydrologic system behaviour requires the ability to characterize the frozen zone at a variety of spatial and time scales. Currently available hydrologic models oversimplify freeze/thaw processes, and will require greater insights into the driving forces between these processes before governing equations can be derived that will facilitate a more physically meaningful level of numerical analysis capabilities (Ireson, 2013). GPR's non-invasive nature and its capacity to monitor these systems over many spatial and time scales makes it highly suited for studying freeze/ thaw cycles.

Chapter 2 of this thesis illustrates the extent to which high resolution GPR can be used to study the complete cycle of seasonal freezing and thawing in temperate climates. The results from the HYDRUS 1-D model facilitated the comparison of the GPR field observations to a numerical simulation to provide some physical constraints to the field data. The main findings of that chapter were:

- High frequency (900 MHz) GPR data can be used to image the interface between the frozen and unfrozen zone (i.e., the BFZ reflection event) and monitor it movement during the winter season.

- GPR profiling found that changes in the reflectivity of the BFZ event appear to correlate with advance and recession of this interface as indicated by the numerical simulation.
- Dispersive diffraction events appear in reflection profiles which indicate the occurrence of thawing in the near surface
- HYDRUS 1-D results correlate well with the GPR-inferred BFZ depths and the near surface thawing dates extracted from CMP soundings and diffraction events respectively

The main findings of this thesis have clearly support the supposition that high resolution GPR is suitable for quantitative characterizing seasonal freeze/thaw cycles. These results can be implemented into other studies to provide useful information regarding winter hydrological processes that were previously challenging to study.

3.2 Recommendation for Future Studies

The purpose of this study was to examine the capacity of surface GPR to characterize seasonal freeze/thaw cycles and clearly demonstrated that GPR data contains information that is consistent with the results of numerical simulations. Additional investigations are required however to further assess the extent to which high frequency surface GPR can be used to increase the state of knowledge regarding the impacts of winter process in temperate zone hydrology. Recommendations for future work include the following:

- An investigation of how EM wave velocities information that can be obtained from surface GPR data can be incorporated in the characterization of freeze-thaw processes. In particular, how can EM wave velocities be used to quantify the ice and liquid water content in the frozen zone.
- A study to examine the nature of the reflectivity change of the BFZ reflection event and what does this change indicate about the conditions at this interface during its advance and recession.
- A further detailed comparison between GPR observations and the results of numerical simulations to determine potential improvements that can achieved in the describing the physical mechanisms involve in winter processes.
- Research on how GPR data can be used to constrain parameters used in the modeling of freeze-thaw processes.

REFERENCES

Baker, T H W, J L Davis, H N Hayhoe, and G C Topp. "Locating the frozen-unfrozen interface in soils using time-domain reflectometry." *Canadian Geotchnical Journal*, 1982: 511-517.

Boike, J, and K Roth. "Time domain reflectometry as a field method for measureing water content and soil water electrical conductivity at a continuous permafrost site." *Permafrost and periglacial procesesses*, 1997: 359-370.

Brooks, R H, and A T Corey. "Hydrualic properties of porous media." *Hydrology papers*, 1964: (March).

Campbell, G S. Soil physics with basic, transport models for soil-plant systems,. New York: Elsevier, 1985.

Carsel, R F, and R S Parrish. "Developing joint probability distributions of soil water retention characteristics." *Water Resource Research*, 1988: 755-769.

Cassidy, N J. "Electrical and magnetic properties of rocks, soil sna dfluids." *In H.M. Jol, (Ed), ground Penetrating Radar: Theory and Applications*, 2009: 41-72.

Chamberlain, E J, and A J Gow. "Effect of freezing and thawing on the permeability and structure of soils." *Engineering Geology*, 1979: 73-92.

Chesworth, Ward. *Encylopedia of soil science.* Spinger, 2008.

Dallimore, S R, and J L Davis. "Ground-penetrating radar investigations of massive ground ice. ." *In Ground Penetrating Radar, Pilon J (ed). Geological Survey of Canada Paper*, 1992: 90-94.

Ding, Y, B Ye, S Liu, Y Shen, S Wang, and M Yang. "Monitoring of frozen soil hydrology in macro-scal in the Qinghai-Xizang Plateau." *chinese Science Bulletin*, 2000: 1143-1144.

Dirksen, C, and R D Miller. "Closed-system freezing of unsaturated soil ." *Soil Science Society of America Journal*, 1966: 168-173.

Duguay, C R, T Zhang, D W Leverington, and V Romanovshy. "Satellite remote sensing of permafrost and seasonally frozen ground." *Remote sensing of Northern hydrology, geophysical monogrph series*, 2005: 91-118.

Fayer, M J. "UNSAT-H Version 3.0: Unsaturated soil water and heat flow model, theory user manual, and examples, ." *Pacific Northwest National laboratory* , 2000.

Fitzhugh, R D, C T Driscoll, P M Groffman, G L Tierney, T J Fahey, and J Hardy. "Efects of soil freezing disturbance on soil solution nitrogen, phosphorus and carbon chemistry in a northern hardwood ecosystem." *Biogeochemistry*, 2001: 215-238.

Flerchinger, G N, and K E Saxon. "Simultaneous heat and water model of freezing snow-residue-soil system I. Theory and development." *Trans ASAE*, 1989: 565-570.

Frauenfeld, O W, T Zhang, R G Barry, and D Gilichinsky. "Interdecadal changes in seasonal freeze and thaw depths in Russia." *Journal of Geophysical Resarch*, 2004.

Gray, D M, P G Landine, and R J Granger. "Simulating infiltration into frozen prairie soils in streamflow models." *Canadian Journal of Earth Sciences*, 1985: 464-472.

Grogan, P.M, C.T Driscoll, T.J. Fahey, J.P. Hardy, R.D. Fitzhugh, and G.L. Tierney. "Colder soils in a warmer world: a snow manipulation study in a northern hardwood forest ecosystem." *Biogeochemistry*, 2001: 215-238.

Hansson, K, J Simunek, M Mizoguchi, L Lundin, and M T van Genuchten. "Water flow and heat transport in frozen soil: Numerical solution and freeze-thaw applications." *Vadose Zone Journal*, 2004: 693-704.

Harris, C, M C Davies, and B Etzelmuller. "The assessment of potential geotechnical hazards associated with mountain permafrost in a warming global climate." *Permafrost and Periglacial Processes*, 2001: 145-156.

Heimann, M, and M Reichstein. "Terrestrial ecosystem carbon dynamics and climate feedbacks." *Nature*, 2008: 289-292.

Henry, H A.L. "Soil freeze-thaw cycle experiments: Trends, methodological weaknesses and suggested improvements." *Soil Biology & Biochemistry*, 2007: 977-986.

Hinkel, K M, et al. "Detection of subsurface permafrost features with ground penetrating radar, Barrow Alaska." *Permafrost and Periglacial Processes*, 2001: 179-190.

Hirota, T, et al. "Decreasing soil-frost depth and its relation to cliate change in Tokachi, Hokkaido, Japan." *J. Meterorol. Soc. Japan*, 2006: 821-833.

Hoekstra, P. "Water movement and freezing pressures." *Soil Scie. Soc. Am. J.*, 1969: 512-518.

Ireson, A M, G van der Kamp, G Ferguson, U Nachshon, and H S Wheater. "Hydrogeological processes in seasonally frozen northern latitudes: understanding, gaps and challenges." *Hydrogeology Journal*, 2013: 53-66.

Iwata, Y, M Hayashi, and T Hirota. "Comparison of snowmelt infiltration under different soil-freezing conditions influenced by snow cover." *Vadose zone Journal*, 2008a: 79-86.

Iwata, Y, M Hayashi, S Suzuki, H Hirota, and S Hasegawa. "Effects of snow cover on soil freezing, water movement and snowmelt infiltration: a paired plot experiment. ." *Water Resource Resources*, 2010: 46.

Jacob, R W, and J F Hermance. "Assessing the precision of GPR velocity and vertical two-way traveltime estimates." *Journal of environmental and Engineering Geophysics*, 2004: 143-153.

Keith, A, D Cherkauer, and P Lettenmaier. "Hydrologic effects of frozen soil in the upper Mississippi River basin." *Journal of geophysical research*, 1999: 19599-19610.

Kneisel, C, C Hanuck, R Fortier, and B Moorman. "Advances in geophysical methods for permafrost investigations." *permafrost and periglacial processes*, 2008: 157-178.

Krzewinski, T G, G T Rupert, and J R Tart. *Thermal design considerations in frozen ground engineering.* Edmonton: ASCE publications, 1985.

LaFleche, P T, A S Jedge, B J Moorman, B Cassidy, and R Bedard. "Ground-probing radar investigations of gravel rosd bed failures, Rae access road, N.W.T., Current Paper Part D." *Geological Survey of Cananada Paper*, 1988: 129-135.

Laxton, S, and J Coates. "Geophysical and borehole investigations of permafrost conditions associated with compromised infrastructure in Dawson and Ross River, Yukon." *Yukon geological Survey*, 2011: 135-148.

Luo, L, et al. "Effects of frozen soil on soil temperature, spring infiltration, and runoff: results from the PILPS 2(d) experiment at Valdai, Russia." *Journal of Hydrometeorology*, 2003: 334-952.

Marlon, G M. *Freeze/thaw processs and soil chemistry.* Special report 95-12, Philadelphia : Army cold regions research and engineering laboratory, 1995.

Moorman, B J. "Ground penetrating radar investigations of woodchip-covered slopes along the Norman Wells pipeline in the Northwest Territories." *Geological Survey of Canada open file 2889*, 1994.

Moorman, B J, S D Robinson, and M M Burgess. "Imaging periglacial conditions with Ground Penetrating radar." *Permafrost and periglacial processes*, 2003: 319-329.

Mualem, Y, and G Dagan. "Hydraulic conductivity of soils: Unified approch to the statistical models." *Soil science society of America Journal* , 1977: 392-395.

Nassar, I N, and R Horton. "Simultaneous transfer of heat, water and solute in porpus media: I theoretical development ." *Soil Science Society of America Journal*, 1992: 1350-1356.

Nelson, F E, A O Anisimov, and N I Shiklomanov. "Subsidence risk from thawing permafrost." *Nature*, 2001: 889-890.

Noborio, K, K J McInnes, and J L Heilman. "Two dimensional model for water, heat and solute transport in furrow-irrigated soil: I. Theory." *Soil Science Society of America*, 1996a: 1001-1009.

Nyberg, L, M Stahli, E Mellander, and K H Bishop. "Soil frost effects on soil water and runoff dynamics along a boreal forest transect: 1. Field investigations." *Hydrological Processes*, 2001: 909-926.

Robinson, S D, B J Moorman, A S Judge, S R Dallimore, and J W Shimeld. "The application of radar stratigraphic techniques to the investigation of amssive ground ice at Yaya Lake, Northest territories, ." *Muskox*, 1992: 39-49.

Rosenzweig, C, et al. "Attributin gphysical and biological impacts to anthropgenic climate change." *Nature*, 2008: 353-357.

Sartz, R. "Soil Water Movement as Affected by Deep Freezing." *Soil Science Society of America Journal*, 1969: 333-337.

Solomon, S, et al. IPCC 2007: Climate change 2007: The physical science basis. Contribution of working group I to the fourth assessment report of the intergovermental panel on climate change 2007. Assessment Report, Cambridge: Cambridge University Press, 2007.

Steelman, C M, A L Endres, and J P Jones. "Hgh-resolution ground-penetrating radar monitoring of soil moisture dynamics: Field results, interpretation, and comparison with unsaturated flow model." *Water Resources Research*, 2012: 1-17.

Steelman, C M, and A L Endres. "An examination of direct ground wave soil moisture monitoring over an annual cycle of soil conditions." *Water Resources Research*, 2010: doi:10.1029/2009WR008815.

Steelman, C, A Endres, and J van der Kurk. "Field observations of shallow freeze and thaw processes using." *Hydrological Processes*, 2010: 2022-2033.

Steelman, C, and T Endres. "Evolution of high-frequency ground-penetrating radar direct ground wave." *Cold Regions Science and Technology*, 2009: 116-122.

Sun, Y, Q Cheng, X Xue, L Fue, J Chai, F Meng, P Schulze Lammers, and S.B. Jones. "Determining in-situ soil freeze-thaw cycle dynamics using an access tube-based dielectric sensor." *Goderma,* 2012: 312-327.

Unger, P W. "Overwinter changes in physical-properties of no-tillage soil." *Soil Science Society of America Journal*, 1991: 778-782.

van der Kruk, J, C M Steelman, A L Endres, and H Vereecken. "Dispersion inversion of electromagentic pulse propagation within freezing and thawing soil waveguides." *Geophysical Research Letters*, 2009: 1-4.

van der Kruk, J, S A Arcone, and L Liu. "fundamental and higher mode inversion of dispersed GPR wave propagating in ice layer." *Transactions on Geoscience and Remote Sensing*, 2007: 2483-2491.

van der Kruk J, Streich R, and Green AG.“Joint dispersion inversion of broadside and endfire CMP georadar data for properties of a thin-surface waveguide.” *Geophysics,* 2006: **71** K19–K29. DOI: 10.1190/1.2168011.

van Genuchten, M Th. "A closed-form equation for predicting the hydraulic conductivity of unsaturated soils." *Soil Science of America Journal*, 1980: 892-898.

Williams, J R, and R O van Everdingen. "Groundwater investigations in permafrost regions of North America: A review." In *North American contribution [to the] second international conference, Volume 2*, 435-446. National Academies, 1973.

Winter, T C. "Relation of streams, lakes and wetlands to groundwater flow systems." *Hydrogeology Journal* (Hydrogeology Journal), 1998: 28-45.

Wolfe, S A. "Massive ice asociated with glaciolacustrine delta sediments, Slave Geological Province, N.W.T., Canada." In Permafrost: Seventh International Conference Proceedings, Lewkowicz AG, Allard M (eds). Centre dètudes Nordiques, Universite Laval, Sainte-foy. Collection Nordicana, 1998: 1133-1139.

Woo, M K, and T C Winter. "The role of permafrost and seasonal frost in the hydrology of northern wetlands in North America." *Journal of Hydrolgoy*, 1993: 5-31.

Woo, M K, P March, and J W Pomeroy. "Snow, frozen soils and permafrost hydrology in Canada, 1995-1998." *Hydrological processes*, 2000: 1591-1611.

Yoshikawa, K, and L Hinzman. "Shrinking thermokarst ponds and groundwater dynamics in discontinuous permafrost near council, Alaska." *Permafrost and periglacial processes*, 2003: 151-160.

Zhang, Y, S K Carey, W L Quinton, R Janowicz, J W Pomeroy, and G Flerchinger. "Comparison of algorithms and parameterisations for infiltration into organic-covered permafrost soils." *Hydrology Earth Systems Sciency*, 2010: 729-750.

Zhang, Y, S Wang, A Barr, and T A Black. "Impact of snow cover on soil temperature and its simulation in a boreal aspen forest ." *Cold region Science Technology*, 2008: 355-370.

Zhao, L, and et al. "Changes of climate and seasonally frozen ground over the past 30 years in Qinghai-Xizang (Tibetan) Plateau, china." *Global Planet*, 2004: 19-31.

Zhao, L, C L Ping, D Yang, G Cheng, Y ding, and S Liu. "Changes of climate and seasonally frozen ground over the past 30 years in Qinghai-Zizang (Tibetan) Plateau, China." *Glabal and Planetary Change*, 2004: 19-31.

Zhao, L, D M Gray, and D H Male. "Numerical analysis of simultaneous heat and mass transfer during infiltration into frozen ground." *Journal of Hyrology*, 1997: 345-363.8

Zhao, L, L Cheng, and S Li. "Changes of plateau frozen-ground and environmental engineering effects. ." *In: The formation environment and development of Qinghai-Tibet Plateau Heibei Science and Technology Press*, 2003: 143-150.